Analysis of the Anisotropies in the Microwave Background Radiation

Carlos Felipe Uribe Muñoz

Presented as a Requirement
to obtain the title of Physicist

Director
Benjamín Oostra

UNIVERSIDAD DE LOS ANDES
FACULTAD DE CIENCIAS
DEPARTAMENTO DE FÍSICA
BOGOTÁ D.C.
November 2007

To my Parents,
and my Sister.

Contents

List of Figures

Preface

This thesis is the final project to culminate four years of hard work in the undergraduate program of Physics. Eventhough I have tried to write as much details as possible, I assume an intermediate knowledge about Physics and specially Cosmology from the reader. For the understanding of Cosmology, the Cosmic Microwave Background Radiation, and demonstrations of useful equations, I have been guided specially by two books written by Andrew Liddle and Marc Lachièze respectively making use of their mathematical notation, and which can be found in more detail in the bibliography of this document.

Some of the results in this paper have been derived using the HEALPix (Górski et al., 2005) package. The project was assisted by M.S. Benjamín Oostra and improved with orientation received by Ph.D. Juan Pablo Negret both of them teachers from the Physics department of *Universidad de los Andes*.

Carlos Felipe Uribe M; Bogotá, Colombia, November, 2007.

Introduction

In this project, you will find the way in which we receive information from the Universe when it only had about 400,000 years of existence after the Big Bang. Chapter 2 shows some theory about Cosmology. On chapter 3, where and how does the Cosmic Microwave Background Radiation comes from will be understanded. Following this, some information about the anisotropies is given. Chapter 7 talks about the data used and provided by NASA, after an explanation of how experimental data is gathered. At the end, there is a Power Spectrum of the Cosmic Microwave Background Radiation from which we can make important conclusions about our universe. Its geometry and the way in which it began are of special interest.

Chapter 1

A Brief History of the Universe

Today, most Physicists accept the Big Bang theory of the formation of the Universe. No one knows exactly why but at the time we define as zero, an amazing explosion took place and with it, all the energy, matter, and space-time were formed. In this process of expansion of the Universe,the energy existing in the vacuum was transformed into what we know. We are certain that the temperature sometime after the Big Bang (exactly at decoupling) was extremely high, of the order of $10^3 K$ as confirmed by the cosmic blackbody radiation we detect today, which leads us to think that the big explosion took place at an even higher temperature. Between 10^{-12} and 10^{-6} seconds after the Big Bang, the Universe continued its expansion and had cooled down so that basic forces of nature appeared as we know them today. Gravity, Strong Force, Weak Force, and Electromagnetic Force appeared in that order respectively. The Subatomic Zoo of elementary particles formed and more complex particles such as neutrons and protons began to form. In the first three minutes of the Universe, protons and neutrons joined together to form the nuclei of light elements. From this time on, until between 300,000 to 500,000 years after the Big Bang, the universe was a hot gas of matter and radiation. Photons scattered on electrons, making the universe opaque. The mean free path of the photons was so short that they could not be considered free until the temperature lowered and electrons combined with the nuclei of Hydrogen and Helium. It was at this moment that photons stopped scattering and today we see them in the microwave spectrum, The Cosmic Microwave Background Radiation. On the following chapters of this project, I will focus on analyzing this radiation that gives us an idea of the universe 300,000 years after the Big Bang.

After 1×10^9 years since the big explosion, some irregularities were seen

in that gas. Gravity pulled together small amounts of this gas creating zones of denser matter; stars began to shine. Since then, until 3×10^9 years of the universe, some galaxies joined together forming elliptical galaxies with a common center with so much gravity that black holes were formed. Some gas enters the black holes but it becomes so hot before it does that it shines and is what we call Quasars. 6×10^9 years after the Big Bang, some of the stars in formation had violent explosions called Supernovae. This explosions are very important because they distribute heavy elements throughout the galaxy.

Our sun was formed in one of the arms of the Milky Way spiral galaxy 5×10^9 years before our present time. Gravity effects made denser amounts of matter from dust around our sun forming the moons, the eight minor planets of our solar system, and asteroids. In about 3×10^9 years from now, the Milky Way Galaxy will crash with a nearby one called Andromeda. Later on, 1×10^{11} years from now, the galaxies will be so far from each other and the universe expanding so fast that not even light will be able to reach from one galaxy to another, and none of them will be seen. We are actually in an era of the universe in which energy generated in the universe comes from fusion of hydrogen and some other elements that takes place in the stars. In the next 1×10^{12} years, this era will be finished and the death of the universe will begin.

1×10^{25} years in the future, the mass of the universe will be concentrated in black holes and neutron stars. The stars will not be burning so the energy in the universe will be generated by particle annihilation and proton decay. After that proton decay, 1×10^{28} years from now, black holes will be what is left of stars and their energy will evaporate slowly. Finally, the universe we know today will end in about these 1×10^{28} years from now when the energy contained in the black holes will be totally evaporated and only neutrinos, positrons, electrons, and photons will be left.

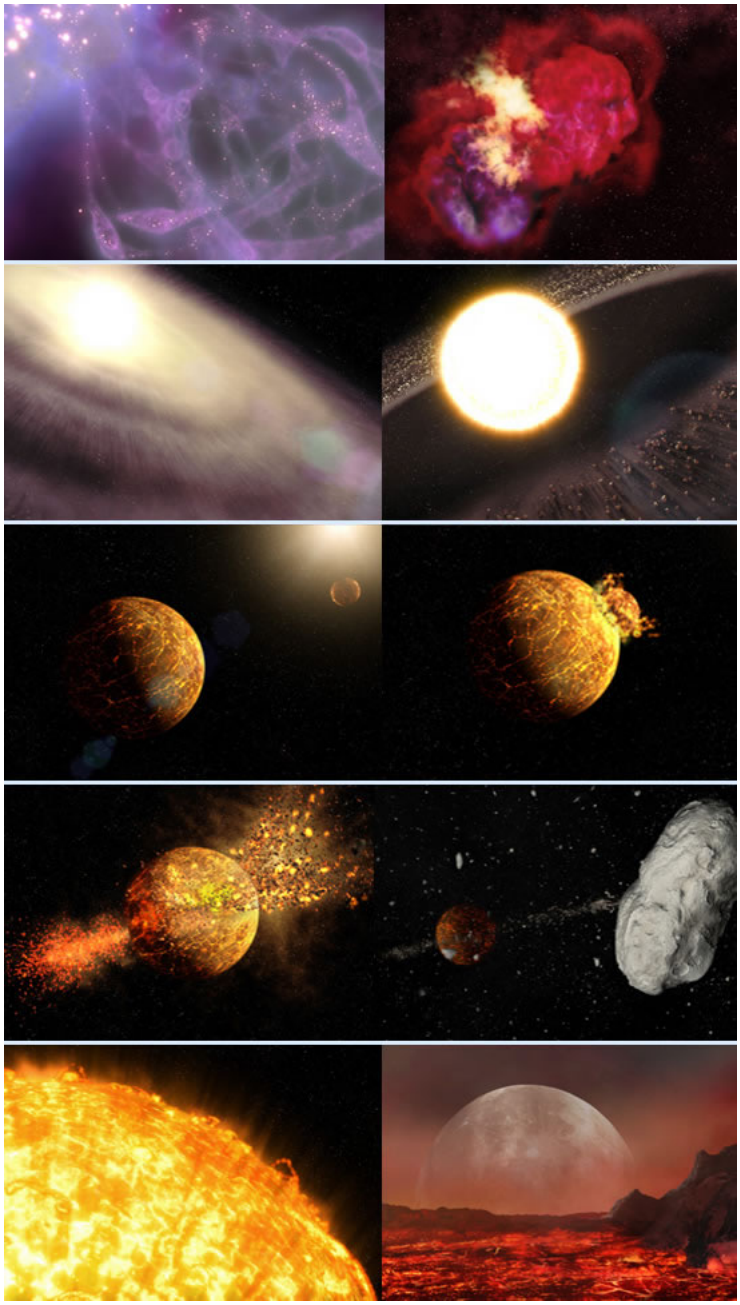

Figure 1.1: The image makes reference to the history of the Universe.[28]

Chapter 2

Important Things About Cosmology

2.1 The Friedmann Equation

The Friedmann equation is the most important equation found in Cosmology. It models the expansion of the universe. It is derived computing the gravitational potential energy and the kinetic energy of a particle, and using conservation of energy which can be seen in more detail in Appendix B. It is important to understand the coordinate system of the comoving coordinates. As the universe expands, these coordinates are taken with the expansion. The relation between the real distance $\vec{r}$ and the comoving distance $\vec{x}$ is given by equation 2.1. *a(t)* is the scale factor of the universe and measures the expansion rate of the universe. It only depends on time because it is assumed that the universe is homogeneous making the same everywhere. Every object in the universe is fixed in the comoving coordinate system and it is the grid that expands with time. Figure 2.1 (taken from reference [10]) shows a very good representation of the comoving coordinate system.

$$\vec{r} = a(t)\vec{x} \tag{2.1}$$

The Friedmann equation expressed in terms of the scale factor is shown in equation 2.2. G is the Newtonian gravitational constant, ρ is the mass density, k is a term that gives the curvature, and c the speed of light. It is important to know that k does not depend on time and it has a constant value in the comoving coordinate system. k is a constant that has units of $[length]^{-2}$.

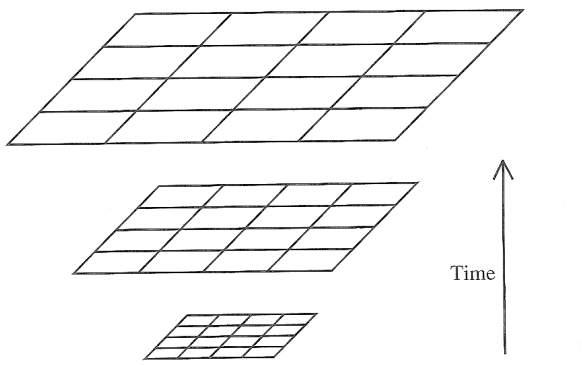

Figure 2.1: Comoving Coordinate System as it expands with time. Note the real distance between point is increasing. [10]

$$\left(\frac{\dot{a}}{a}\right)^2 = \frac{8\pi G\rho}{3} - \frac{kc^2}{a^2} \tag{2.2}$$

2.2 About Geometry of the Universe

The universe can have three types of "geometries";flat, spherical, or hyperbolic. A flat universe is based on Euclidean Geometry and it follows then that the sum of the angles of a triangle add up to $180°$ and that the circumference of a circle is given by $c = 2\pi r$ being c the circumference and r the radius of the circle. A spherical universe is described by another type of geometry in which the angles of the triangle add to more than $180°$ and the circumference of the circle is less than that given by Euclidean Geometry. Finally, the hyperbolic Universe is one in which the angles of the triangle add up less than $180°$ and the circumference of a circle is greater than $2\pi r$. A better idea of this description can be achieved by taking a look at figure 2.2.

In the Friedmann Equation, the three possible geometries of the universe are described by the value of k (that is why it is called the curvature term). If $k = 0$ the universe is a flat universe. If $k > 0$ the universe is a spherical universe and it is said to be a closed universe. Finally, if $k < 0$ it is a hyperbolic universe and it is said to be an open universe. Notice the importance of the Friedmann equation

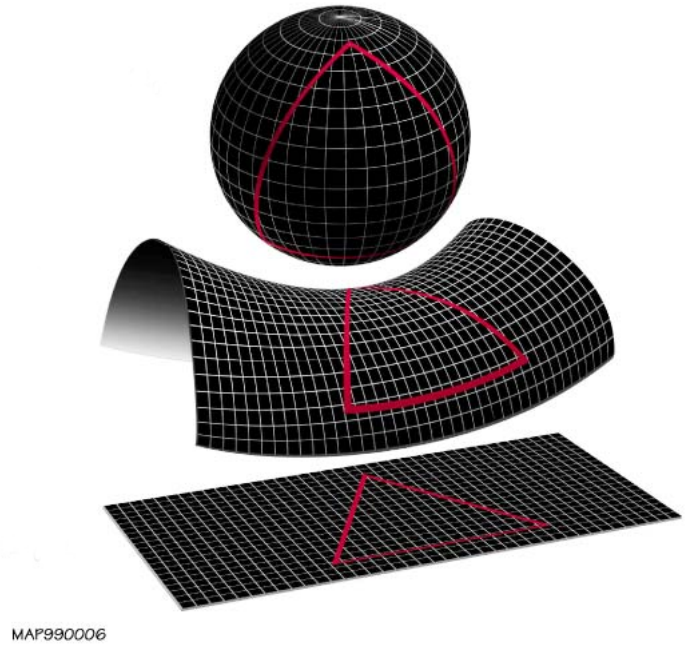

Figure 2.2: The possible shapes of the universe. At the top the spherical geometry, hyperbolic in the middle, and flat at the bottom. [29]

and all the information it gives about the geometry of the universe.

2.3 Fluid and Acceleration Equations.

The density term in the Friedmann equation must also be described to get a complete understanding of the universe. Using the first law of thermodynamics, rearranging terms and taking into account a reversible process (expansion), equation 2.3 is obtained and it is called the Fluid Equation. It describes how the density of the material in the universe is changing with time. In this equation the new term that appears is p and it is the pressure of the material. This equation is derived in appendix B in a better detail.

$$\dot{\rho} + 3\frac{\dot{a}}{a}\left(\rho + \frac{p}{c^2}\right) = 0 \tag{2.3}$$

From the fluid equation, it can be seen that the density of the material in the

universe (it can be matter or radiation) changes because of the volume change as the universe expands or by the pressure of the material that makes work as the expansion takes place.

Using the Friedmann and the Fluid equation, a third equation can be stated that is not independent of these two. It is called the acceleration equation and it gives information about the acceleration of the scale factor. Equation 2.4 shows this and it can be seen that if the material of the universe has any pressure it decelerates the expansion.

$$\frac{\ddot{a}}{a} = \frac{-4\pi G}{3}\left(\rho + \frac{3p}{c^2}\right) \tag{2.4}$$

2.4 Hubble Law and the Friedmann equation

Hubble found out that the velocity at which galaxies are receding from one another is proportional to the distance and it's given by the Hubble Law shown in equation 2.5 where H is known as the Hubble parameter.

$$\vec{v} = H\vec{r} \tag{2.5}$$

The velocity is given by $\vec{v} = \frac{d\vec{r}}{dt}$ and it goes in the direction of the vector $\vec{r}$. So using this fact and the one shown in equation 2.1 it can be written as shown in equation 2.6 letting us say that the Hubble parameter is $H = \frac{\dot{a}}{a}$.

$$\vec{v} = \frac{\dot{a}}{a}\vec{r} \tag{2.6}$$

The Friedmann equation can be written in terms of the Hubble parameter as shown in equation 2.7. The Hubble parameter is then not constant in time because it depends on the scale factor and the rate of expansion.

$$H^2 = \frac{8\pi G\rho}{3} - \frac{k}{a^2} \tag{2.7}$$

2.5 The Expansion and the Redshift of Emitted Light.

The redshift is defined as shown in equation 2.8 where λ makes reference to the wavelength of a certain wave and the subscripts obs and em tell whether is observed or emitted respectively.

$$z = \frac{\lambda_{obs} - \lambda_{em}}{\lambda_{em}} \tag{2.8}$$

From equation 2.6 one knows that $dv = Hdr$ and applying the Doppler Law shown on equation 2.9 where v_r is the receding velocity, c the speed of light, and the subindexes obs and em make reference to the wavelength observed and emitted respectively, equation 2.10 is obtained.

$$v_r = c\frac{\lambda_{obs} - \lambda_{em}}{\lambda_{em}} \tag{2.9}$$

$$\frac{d\lambda}{\lambda_{em}} = \frac{da}{a} \tag{2.10}$$

Integrating this equation tells us the very important relation that $\lambda \ \alpha \ a$. Using the redshift as defined in equation 2.8 it can be related to a as shown in equation 2.11 where t_{em} is the time in which light was emitted and t_{obs} the time at which that light is observed.

$$1 + z = \frac{a(t_{obs})}{a(t_{em})} \tag{2.11}$$

2.6 Solving Fluid Equation for Matter and Radiation.

Matter is considered as a material which pressure is zero and in this case as non relativistic too. Using the Fluid Equation, stating that $p = 0$, and that the present matter density is ρ_0 the obtained result is shown in equation 2.12.

$$\rho_{matter} = \frac{\rho_0}{a^3} \tag{2.12}$$

In the case of radiation, there is a pressure $p = \rho_{rad}c^2/3$ and solving the Fluid Equation the obtained result is shown in equation 2.13.

$$\rho_{rad} = \frac{\rho_0}{a^4} \tag{2.13}$$

In the case of matter the density falls as the inverse of the volume as expected. In radiation, density falls faster. The universe is of course a mixture of radiation and matter but in most epochs one of the two will be dominant.

2.7 About H_0 and the Relative Density Ω_0

The Hubble parameter is not well known so it is usually presented as a function of an adimensional parameter h. The subscript "0" indicates that this is the present value of H because H isn't constant in time. It is called ´´constant" because it has the same value for many galaxies.

$$H_0 = 100hkms^{-1}Mpc^{-1} \tag{2.14}$$

Actually the Hubble Space Telescope Key Project has measured an actual value of $h = 0.72 \pm 0.08$.[1] With this parameter the distance to many objects can be well determined from their redshifts.

Another important parameter is Ω defined as the fraction of density to a critical density of the universe as seen in equation 2.15.

$$\Omega = \frac{\rho}{\rho_c} \tag{2.15}$$

The critical density ρ_c is the density that makes k in the Friedmann equation equal to zero. It is easy to see that

$$\rho_c = \frac{3H^2}{8\pi G} \tag{2.16}$$

The critical density changes with time because H changes with time. However, the present critical density can be computed obtaining the value:

$$\rho_c(t_0) = 1.88h^2 \times 10^{-26}kg \cdot m^{-3} \tag{2.17}$$

It is commonly expressed in units of solar masses and it has the value:

$$\rho_c(t_0) = 2.78h^{-1} \times 10^{11}M_\odot/(h^{-1}Mpc)^3 \tag{2.18}$$

Now in terms of the new Ω, the Friedmann equation can be written as shown in equation 2.19.

$$H^2 = H^2\Omega - \frac{k}{a^2} \tag{2.19}$$

From this equation one can say that

[1] Liddle Andrew, An Introduction to Modern Cosmology, Wiley, Second Edition, pg. 46.

$$\Omega - 1 = \frac{k}{H^2 a^2} \tag{2.20}$$

which can help to determine the geometry of the universe if Ω is known.

2.8 Adding a Cosmological Constant

A new term can be added to the Friedmann equation as shown in equation 2.21

$$H^2 = \frac{8\pi G\rho}{3} - \frac{k}{a^2} + \frac{\Lambda}{3} \tag{2.21}$$

The introduction of such a term is permitted by general relativity, and although Einstein's original motivation has long since faded, it is currently seen as one of the most important and enigmatic objects in cosmology.[2]

In this equation, the cosmological constant has units of $[time^{-2}]$

The acceleration equation can also be rewritten with a new term involving the cosmological constant as shown in equation 2.22.

$$\frac{\ddot{a}}{a} = \frac{-4\pi G}{3}\left(\rho + \frac{3p}{c^2}\right) + \frac{\Lambda}{3} \tag{2.22}$$

As done some sections ago, the Friedmann equation can be rewritten in terms of Ω_Λ as shown in equation 2.23, in which $\Omega_\Lambda = \frac{\Lambda}{3H^2}$.

$$\Omega + \Omega_\Lambda - 1 = \frac{k}{a^2 H^2} \tag{2.23}$$

Restrictions about geometry of the Universe can be given and they follow that:

- If $\Omega + \Omega_\Lambda$ is between zero and 1, then the universe is an open universe.
- If $\Omega + \Omega_\Lambda$ is equal to 1, the universe has a flat geometry.
- If $\Omega + \Omega_\Lambda$ is greater than 1, the universe would have a spherical geometry making it a close universe.

[2]Liddle Andrew, An Introduction to Modern Cosmology, Wiley, Second edition, pg. 51.

Chapter 3

Dipole Anisotropy due to Earth's Kinematics

3.1 First Approach to the Cosmic Microwave Background

Photons follow a Planck black body spectrum distribution at a certain temperature T that has an occupation number η given by equation 3.1. In this case h is the Planck constant, k_b is Boltzmann constant, and f the frequency of the photon. This is the occupation number per mode due to the possible polarizations of the photons.

$$\eta = \frac{1}{exp(hf/k_bT) - 1} \tag{3.1}$$

By taking a look at equation 3.1, one can notice that if $hf >> k_bT$ there will be few photons. If $hf << k_bT$ one finds many photons in that state. Taking this into account and knowing that the energy of one photon is given by $E_{photon} = hf$ it is better to find out how are the energy states distributed. The energy density ϵ, defined as the energy per unit volume, depends on the frequency of the photon and follows equation 3.2 showing how energy is distributed at different frequencies. Figure 3.1 shows the behavior of this distribution in which the peak is found when hf/k_bT is near 2.8.

$$\epsilon(f)df = \frac{8\pi h}{c^3}\frac{f^3 df}{exp(hf/k_bT) - 1} \tag{3.2}$$

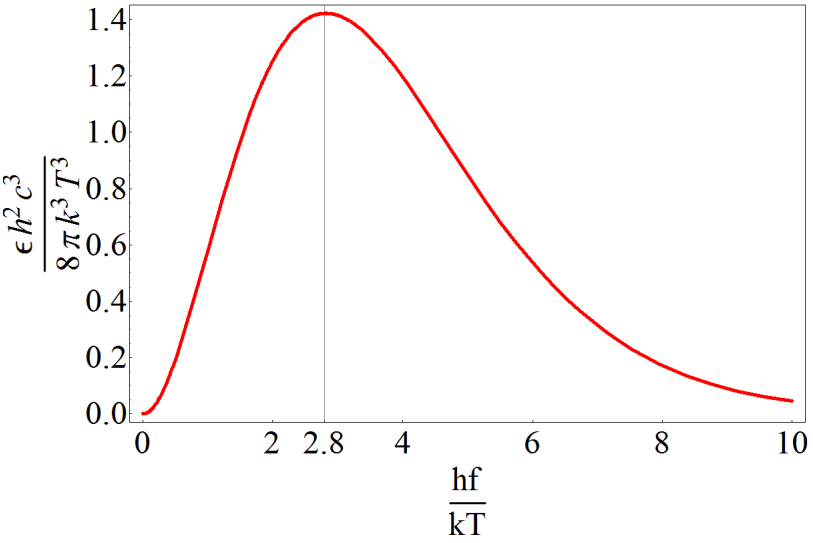

Figure 3.1: The Blackbody Energy Density Distribution

Integrating equation 3.2 one can get to the result shown in equation 3.3 which gives the total radiation energy density and this shows it is proportional to T^4, where $\alpha \equiv \frac{\pi^2 k_b^4}{15\hbar^3 c^3}$.

$$\epsilon = \rho_{rad} c^2 = \alpha T^4 \tag{3.3}$$

Today we know that the Cosmic Microwave Background Radiation follows a Black-Body spectrum distribution at an average temperature of $T_0 = 2.725 \pm 0.001K$[1] Using equation 3.3 and 2.13 it can be shown that the temperature of the universe decreases as the universe expands as shown in equation 3.4 and in which $\beta \equiv \left(\frac{\rho_{0rad} c^2}{\alpha}\right)^{\frac{1}{4}}$.

$$T = \frac{\beta}{a} \tag{3.4}$$

The temperature change with the expansion should then change the distribution of the Black Body Spectrum of the photons in the early universe. However, this evolution conserves the shape of the Black Body spectrum because the frequency of light reduces by a factor of $\frac{1}{a}$ too. The exponential in equation 3.2

[1]Liddle Andrew, An Introduction to Modern Cosmology, Wiley, Second Edition, pg. 75.

depends on the frequency and the Temperature canceling this effect. The cube of the frequency will then make the energy density decrease as the inverse of the volume; that is exactly what is supposed to happen. The distribution continues to be a black-body spectrum distribution but with a different temperature. Figure 3.2 shows how this evolution happens.

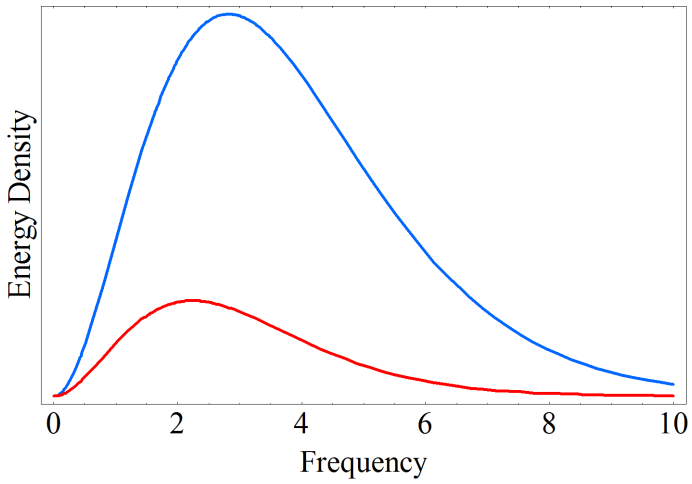

Figure 3.2: The Blackbody Energy Density Distribution for the Microwave Background Radiation at two different moments of the universe. The red graph is some time later when the universe has expanded compared to the moment in which the photons showed the blue spectrum.

On the next section you will find information about the origin of the CMBR and get a better understanding of it.

3.2 The Surface of Last Scattering

During the recombination period of the history of the Universe, when the temperature was low enough so that electrons were captured by the nuclei of the elements, photons stopped being scattered. Before recombination, we do not have any information about the universe in electromagnetic waves.[2] Recombination is the point of history where we begin to receive information of the young universe in

[2]Neutrinos and Gravitational Waves give us information of the Universe before this time, but we haven't detected them yet.

the form of electromagnetic waves. Recombination follows equation 3.5 in which a proton captures an electron and the result is a hydrogen atom and a free photon.

$$p^+ + e^- \rightarrow H + \gamma \tag{3.5}$$

The Hydrogen atom has a minimum ionization energy of 13.6 eV. The mean free path of the photons was short at the beginning of the universe, but as the universe expanded and cooled down, the photons lost energy until they were not being able to ionize the atoms. Finally the decoupling period was achieved in which the photons stop being scattered and so the universe begins to be transparent.

All of these free photons travel toward us with the speed of light c and all of them have been traveling the same distance, d_{tr} until they reach our detectors today. Equation 3.6 describes this amount as known from classical kinematics without taking into account a universe expansion. In this equation t_{tr} is the time the photons have been traveling toward us.

$$d_{tr} = c(t_{tr}) \tag{3.6}$$

Space-time geometry makes equation 3.6 a little more complex. To treat this, we imagine a spherical surface, see figure 3.3, in which we are located in the center of the sphere. All the photons come from that surface toward us meaning that they travel the same distance, which value is the radius of the sphere d_{tr}.This spherical surface is what we call the ´´Surface of Last Scattering" which we think of as the source of all the Cosmic Microwave Background Radiation.

To determine the temperatures at which recombination and decoupling happened, the Saha equation 3.7 is used. χ is defined as the ratio between the density of photons and the density of baryons, and it is called the ionization fraction. Only hydrogen is taken into account in the Saha equation, it takes the ratio of photons to baryons and their distribution functions.

$$\frac{1-\chi}{\chi^2} \approx 3.8 \frac{n_B}{n_\gamma} \left(\frac{k_b T}{m_e c^2} \right)^{\frac{3}{2}} exp\left(\frac{13.6eV}{k_b T} \right) \tag{3.7}$$

A way of defining recombination is when $\chi = 0.1$ that means when 90% of the electrons are combined with the protons. Solving the Saha equation then

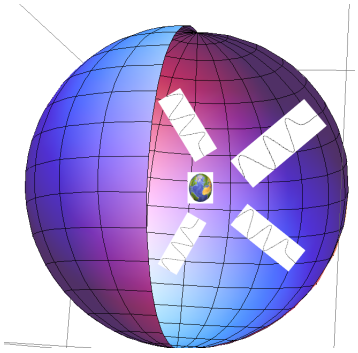

Figure 3.3: Diagram of the Earth inside the Surface of Last Scattering receiving the Photons.

gives $T_{rec} = 3600K$. A similar way of finding the temperature of decoupling, is defining the mean free path of the photons as the age of the universe and then $T_{dec} = 3000K$ is obtained. With this data, it is easy to calculate z (the redshift) of the photons in decoupling. Using equation 2.11 and equation 3.4, and taking $a_0 = 1$ as the scale factor today, the obtained value is shown in equation 3.8.

$$z_{dec} = \frac{a_0}{a_{dec}} - 1 = \frac{T_{dec}}{T_{today}} - 1 \approx 1100 \tag{3.8}$$

This means that the photons we see today have a wavelength of about 1100 times greater than at the time they were at the surface of last scattering. Using Wien's law shown in equation 3.9 with the constant $b = 2.898 * 10^{-3} mK$ the wavelength of the photons at decoupling was about 966 nm. This puts the photons at decoupling in the infrared part of the electromagnetic spectrum. The photons we see today have a wavelength of about 1060 μm which moves the photons to the far infrared part of the spectrum called the microwaves. An illustration of the electromagnetic spectrum is shown in figure 3.4

$$\lambda = \frac{b}{T} \tag{3.9}$$

Finally to close this section, it is important to know that in the young universe the only elements produced were hydrogen because it is the most stable light nucleus, and helium because some protons were left over and there were not enough neutrons for each one.

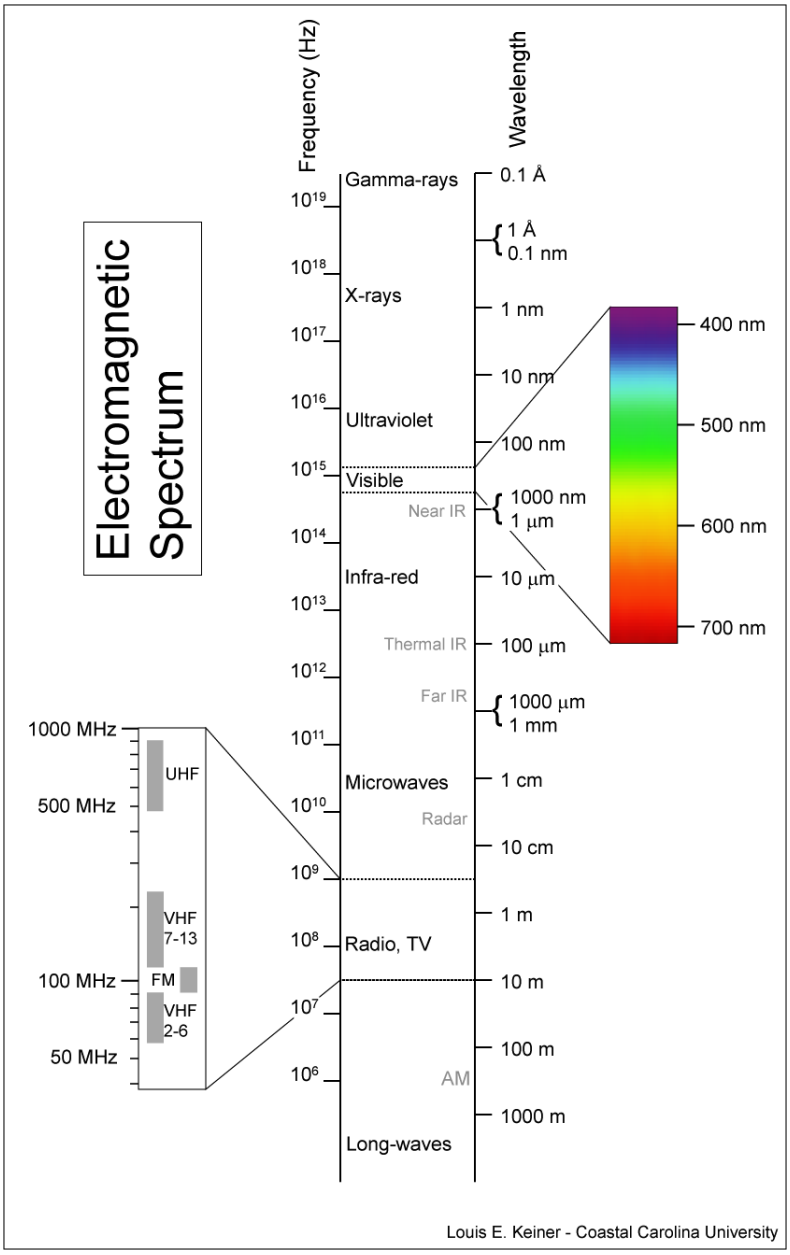

Figure 3.4: Diagram of the electromagnetic spectrum.[30]

3.3 Mathematical and Physical concepts in the Dipole anisotropy

Appendix A shows how the Cosmic Microwave Background Radiation (CMBR) map can be treated as a decomposition in spherical harmonics. Almost all of the dipole anisotropy has to do with the Doppler Effect due to the velocity $\vec{V}$ of the solar system with respect to the surface of last scattering. The dipole is given by a vector $\vec{d}$ such that equation 3.10 is satisfied with $\hat{q}$ a direction, a_{1m} a coefficient and Y_{1m} spherical harmonics.

$$\vec{d}(\hat{q}) \equiv \sum a_{1m} Y_{1m}(\hat{q}) \tag{3.10}$$

In celestial coordinates,shown in figure 3.5, being α the right ascension and δ the declination, a cartesian coordinate system can be established so in a first approximation the Doppler Effects due to $\vec{V}$ is given by $\vec{d} = \frac{\vec{V}}{C}$ and is then presented in three components T_x,T_y,and T_z. The temperature correction of the sky is then given by equation 3.11 where T_0 was the temperature assuming Earth was not moving with respect to the Surface of Last Scattering.

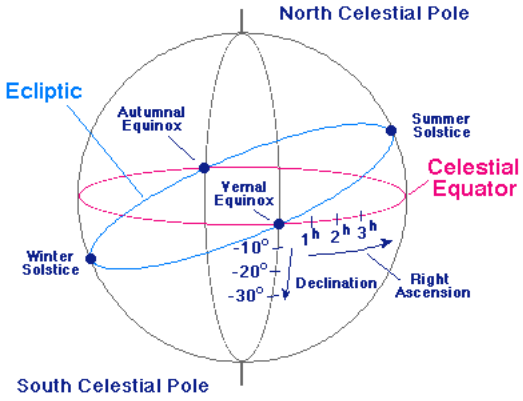

Figure 3.5: Celestial Coordinates System[3]

$$T(\alpha, \delta) = T_0 + T_x Cos(\delta) Cos(\alpha) + T_y Cos(\delta) Sin(\alpha) + T_z Sin(\delta) \tag{3.11}$$

Until now, the dipole anisotropy has been treated as if all the points on the Last Scattering Surface were moving away from the observer at the same radial

speed. Of course this is not completely correct and a cosmological point of view is needed for the treatment of the problem.

3.4 The Cosmological Point of View

If the observer on Earth is located at the center of the Surface of Last Scattering, he would see a shift z_{obs} in all directions of the sky. If no intrinsic anisotropies are taken into account, a temperature $\frac{T_{obs}}{Z_{obs}}$ would be measured in all the different directions.

The Earth is in fact moving with velocity $\vec{V}$ with respect to the Last Scattering Surface. The Doppler effect causes a shift in the frequency proportional to the velocity of Earth that depends on the direction of movement and the portion of the sky being observed. When all these facts are applied to a black-body spectrum, equation 3.12 is obtained. θ is the angle between the direction of observation and the direction of the velocity of Earth.

$$T(\theta) = \frac{T_0(1-V^2)^{1/2}}{1 - VCos(\theta)} \tag{3.12}$$

The velocity of the dipole is said to be $365 \pm 18 Km/s$ in the direction $l = 265°$ $b = 48°$ in the plane of the sky. The Earth moves respect to the Sun with a speed of $20 Km/s$ toward $l = 57°$ $b = 23$. It is also moving with respect to the center of the Milky Way with a speed of $220 Km/s$ at $l = 90°$ $b = 0°$. The whole galaxy is moving with respect to the CMBR at a speed of $550 Km/s$ toward $l = 266°$ $b = 30°$. Our Sun is moving with respect to the local group at a speed of $308 Km/s$ toward $l = 107°$ $b = -7°$. Finally, our local group is moving with respect to the CMBR at a speed of $620 Km/s$ toward $l = 277°$ $b = 30°$.[3] This speed is much smaller than c so making a Taylor expansion terms of order greater than 1 in V can be neglected as long as V is expressed in units of c. The expansion is shown in equation 3.13.

$$T(\theta) \approx T_0(1 + VCos(\theta)) \tag{3.13}$$

[3]Gurzadyan V. G., Kocharyan A. A. Paradigms of the Large-Scale Universe, CRC Press, 1994. Pg.10. Available in electronic form at http://books.google.com/books?id=4cIcmQfeSYEC&printsec=frontcover&dq=Paradigms+of+the+Large-Scale+Universe&hl=es&sig=6LtNine1hryPCY4Z5hnliiLwQFg#PPP1,M1

The term that includes $Cos(\theta)$ is the one due to the dipole. When the temperature is measured in the direction of the Earth's velocity, a shift towards blue is measured, while in the opposite direction the measured shift is red. In other directions, the effect is intermediate between this two.

Chapter 4

Intrinsic Anisotropies

4.1 Intrinsic Thermal Anisotropies and relation between spatial and angular scales.

Models of the Big Bang predict that the surface of last scattering should be homogenous with the same density and temperature. According to this, it is expected to have an isotropic CMBR. The origin of this radiation is the surface of last scattering so it should be the same no matter in which direction the observer is looking. With all this in mind, it seems strange that intrinsic fluctuations have appeared even before the time of recombination. Isotropy means that when measurements of the intensity (or temperature) of the radiation are made, the same result is obtained in all directions. We have been able to figure out some types of this intrinsic fluctuations.

The first of these fluctuations is a thermal one. In this case the black-body spectrum of the CMBR is not modified but variations in the intensity of it are detected as a function of the direction being observed. The intensity of the radiation is related to a temperature, and the fluctuations of $\frac{\Delta T}{T}(\hat{q})$ are usually shown as the mean difference of this expression in directions separated by an angle θ.

A fluctuation of the CMBR in the time of recombination is given by a spatial scale. Today we describe anisotropies using an angular scale expressed in spherical harmonics (see appendix A). When we observe the CMBR today, we look at the sky but we see a projection of the surface of last scattering (a sphere) on our two-dimensional sky. An expression that gives a relation between these

two scales is necessary to describe fluctuations in density. Comoving units are used to do this job. The surface of last scattering has a thickness too because all these processes didn't occur instantaneously. This means that we have to take into account a time scale too because some of the fluctuations we detect today could have their origin at different times. A relation between the spatial scale and the angular scale is shown on following chapters when analyzing the power spectrum.

4.2 Anisotropies due to matter density.

When radiation is emitted or scattered by matter, a Doppler shift appears depending on its velocity. Matter also creates a gravitational field that causes a redshift in the radiation. Most of the models of galaxy formation talk about density fluctuations even before recombination that cause this type of fluctuations in the CMBR.

All these effects are the origin of intrinsic anisotropies of the CMBR. It is important to determine what type of statistics do this anisotropies follow. Most of the models assume the Gaussian statistics that is completely determined by the power spectrum of the fluctuations. Knowing the spectrum and the statistics it follows, we can predict fluctuations that can be seen today eventhough it is sometimes very complex and it depends of the model used. Without taking into account any possible re-ionization, anisotropies of the type $\frac{\Delta T}{T}$ must have been survived until today. On the other hand, the anisotropies due to the fluctuations in matter density evolved since recombination giving origin to galaxies and other great scale structures.

At very large angular scales, a great part of the fluctuations is due to a gravitational effect. The photons scattered in a region where the gravitational potential is different from zero, gain a redshift according to general relativity. This fluctuation is called the Sachs-Wolfe effect. A fluctuation in density will cause a fluctuation in the gravitational potential. When we observe the scattered or emitted photons, we find they come from a zone in which there is a difference in the gravitational potential with respect to us. The redshift that those photons gain depends on the gravitational potential. By definition, the fluctuation of the gravitational potential is said to be zero when the curvature is constant. In this case, a fluctuation in the temperature can still be caused by an entropy change.

Chapter 5

$\Omega' s$ in the Universe and Inflation

Equations 2.17 and 2.18 give the value of the critical density of the universe. Knowing this, people have calculated values for different $\Omega' s$ including density ratios for stars, baryons, and halos around galaxies. Knowing a star's luminosity and temperature lets us calculate their mass. Doing this the density of stars in the universe can be measured to a good estimate and Ω_{stars} can be known. Using other methods, Baryonic density can also be calculated, and to a good estimate Ω_B can be known too. By taking a careful look at galaxy dynamics, we are able to estimate a density of matter we cannot see but it is supposed to be around the galaxies and then we can know the value of Ω_{halo}. Table 5.1 shows their accepted values or constrictions already made.

Ω
$\Omega_{stars} \approx 0.01$
$0.016 \leq \Omega_B h^2 \leq 0.024$
$\Omega_{halo} \approx 0.1$

Table 5.1: Values or constraints for $\Omega' s$.

In general, many experiments have taken us to take a value of Ω_0 which is the value of the density ratio for all the matter of the universe, to be $\Omega_0 > 0.2$. All the matter we know is a very small percentage of the total density, there is another type of matter we call dark matter because we cannot see it, but that is subject for another discussion and I will not talk about it in this project.

We know well that $\Omega_{total} = \Omega_0 + \Omega_\Lambda$ has the restriction shown in equation 5.1.

$$0.5 \leq \Omega_{total} \leq 1.5 \tag{5.1}$$

Some results of the Big Bang theory were not completely satisfactory which lead to the introduction of what we know by Inflation. First of all, from the Friedmann equation, we know that a flat universe remains flat meaning Ω_{tot} is very close to one. However, by solving the Friedmann equation of what we know about the densities (radiation and matter) as given by equations 2.12 and 2.13 the term $\Omega_{tot} - 1$ would change with time meaning that the curvature of the universe changes with time. There's another problem that has to do with the horizon and the origin of the cosmic microwave background radiation. Eventhough we detect some anisotropies in it, the microwave background radiation is very close to being isotropic. This means that in the past, points in the sky almost reached a thermal equilibrium. If we think as the visible universe being the size of a distance light has traveled in a certain direction, if those photons of the CMBR are just reaching us, then points in the universe that we see in the sky at opposite directions would have not been able to interact to reach this. Andrew Liddle has a very good representation of this which you can see in figure 5.1.

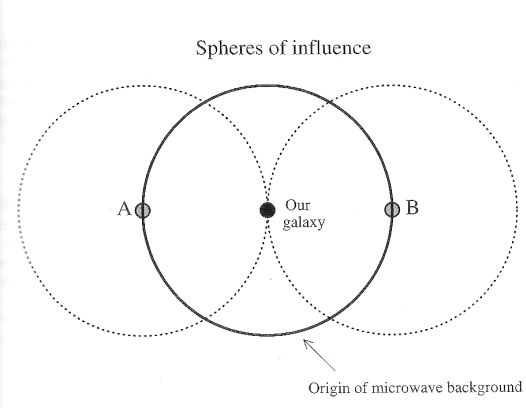

Figure 5.1: Points A and B cannot interact to reach the thermal equilibrium.[10]

Due to these problems, Alan Guth in 1981 began to talk about inflation. During inflation, the scale factor is accelerating meaning that $\ddot{a} > 0$. Taking a look at equation 2.4 implies equation 5.2 which gives a negative pressure because $\rho > 0$.

$$p < \frac{-\rho c^2}{3} \tag{5.2}$$

In the Friedmann Equation with the cosmological constant as shown in the equation 2.21 , the first two terms can be neglected compared with the third because they decay very fast as the expansion happens. Solving for a equation 5.3 is obtained.

$$a(t) = exp\left(\sqrt{\frac{\Lambda}{3}}t\right) \tag{5.3}$$

Inflation ends when the energy contained in Λ converts to mass, and matter is formed. Inflation is supposed to occur in the first 10^{-34} s after the big explosion.

Looking at the Friedmann Equation 2.20, what inflation does is keeping the denominator at the right side to be greater than zero and keeping Ω_{tot} close to one. Inflation then predicts a flat universe.

Chapter 6

NASA's WMAP Mission

WMAP means *Wilkinson Microwave Anisotropy Probe* name given to honor Dr. David Wilkinson who was a very important member of the science team that proposed to study the microwave background radiation. NASA received the WMAP idea in 1995. One year later, it was selected as a mission administered by the Explorers Program. It was on June 30 of 2001 when the observatory was launched from Cape Canaveral to space. [18, 19]

The WMAP makes differential measurements of the sky. You can see in figure 6.1 that the top part of the observatory is cooled by some radiator plates. On the bottom, it has a shield that protects the probe from radiation originated on Earth and/or the Sun.

WMAP was constructed to measure the relative CMBR temperature over the full sky with resolutions never seen before, and improving the COBE's (an older NASA shuttle used to gather CMBR data) obtained results.

WMAP was built to gather information about the relative temperature of the Cosmic Microwave Background Radiation. WMAP is able to take measurements on all the sky and it has an angular resolution of 0.3°. It can detect temperature fluctuations of 20 μK per 0.3° square pixel.

The WMAP probe is located in the L2 Sun-Earth Lagrange point as shown in figure 6.2 where it can point away from the Sun and the Moon to acquire data.

The WMAP has 10 feeds distributed in the following way in order to detect

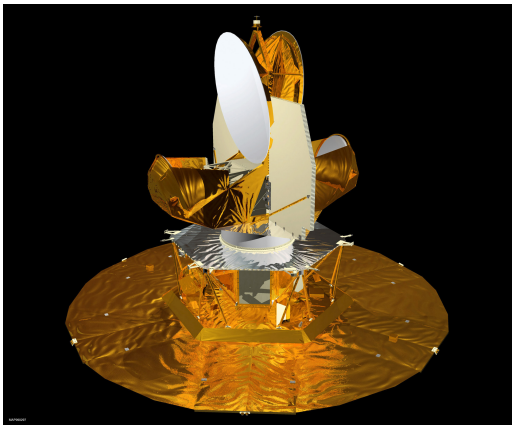

Figure 6.1: WMAP spacecraft [17]

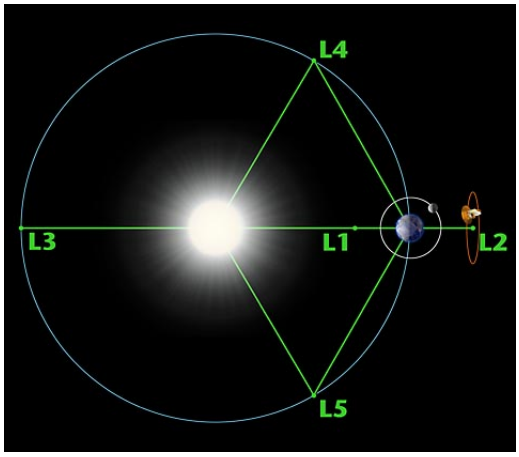

Figure 6.2: Lagrange points between Earth and Sun[22]

intensity.

- One pair in the K band.
- One pair in the Ka band.
- Two pair in each of the Q and V bands.
- Four pair in the W band.

Signals received from each pair of feeds form a total of ten differential assemblies. Each assembly gives information that depends on a temperature difference of two points at certain directions on the sky. The different frequencies for each band are shown in table 6.1.

Band	K	Ka	Q	V	W
Frequency (GHz)	23	33	41	61	94

Table 6.1: Frequency Bands [20]

People from NASA used these frequencies based on several things. The smallest frequency should be 22 GHz because frequencies lower than this one can be measured from Earth. In order to reduce a certain type of noise, which is described in chapter 7, they decided to have a maximum frequency of 100 GHz. Intermediate frequencies were chosen to have those values because actual technology could then be used to develop the detectors and gather the data for the analysis easily.

The WMAP has two symmetric telescopes producing two focal planes located at opposite sides on a symmetry axis of the probe. The ten feeds are located in each focal plane, and the idea of using more of these at higher frequencies is to reduce noise that can be higher at those elevated frequencies. Figure 6.3 shows the localization of these feeds on the two focal planes.

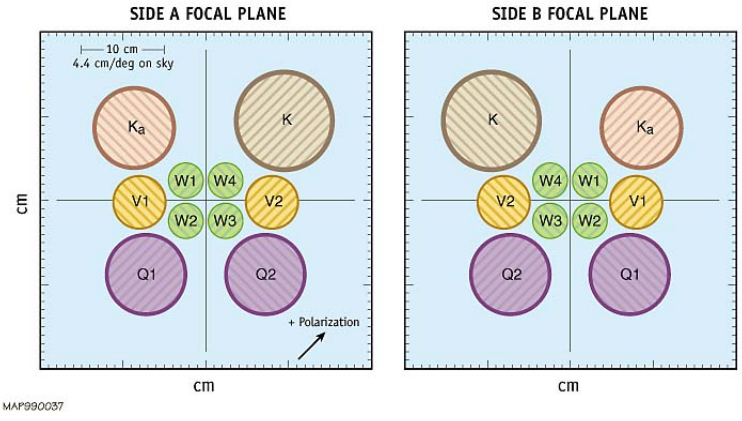

Figure 6.3: Localization of the feeds in the focal planes. [21]

Each pair of feeds constitute a differential assembly, the condition is to be measuring in the same frequency. The output depends on how bright is the difference between the temperature, which is detected depending on how bright a certain direction is, between the two directions being observed.

WMAP has to cover all the sky so a low order spherical harmonic moment can be well determined. The anisotropy probe covers all the full sky every six months, making the data to have more than just one measurement in the years it has been collecting it. To maintain sensitivity at large angular scales, the angular separation of the points at which the difference is taken must be large. Eventhough the separation for the different channels can be different, the two lines of sight are separated by about 141°. The temperature given by the WMAP for each pixel is the average of all observations of that pixel. It is important to observe each pixel with the greater number of neighboring pixels around to get a better statistical value of the temperature of it.

A more detailed information about the WMAP satellite is shown in figure 6.4 which has been provided by NASA.

WMAP Mission Characteristics:

	K-Band[a]	Ka-Band[a]	Q-Band[a]	V-Band[a]	W-Band[a]
Wavelength (mm)[b]	13	9.1	7.3	4.9	3.2
Frequency (GHz)[b]	23	33	41	61	94
Bandwidth (GHz)[b, c]	5.5	7.0	8.3	14.0	20.5
Number of Differencing Assemblies	1	1	2	2	4
Number of Radiometers	2	2	4	4	8
Number of Channels	4	4	8	8	16
Beam Size (deg)[b, d]	0.88	0.66	0.51	0.35	0.22
System Temperature, *Tsys* (K)[b, e]	29	39	59	92	145
Sensitivity (mK sec$^{1/2}$)[b]	0.8	0.8	1.0	1.2	1.6

Sky Coverage	Full sky
Optical System	Back-to-Back Gregorian, 1.4 x 1.6 m primaries
Radiometric System	Differential polarization sensitive receivers
Detection	HEMT amplifiers
Radiometer Modulation	2.5 kHz phase switch
Spin Modulation	0.464 rpm = ~ 7.57 mHz spacecraft spin
Precession Modulation	1 rev hr^{-1} = ~ 0.3 mHz spacecraft precession
Calibration	In-flight: amplitude from dipole modulation, beam from Jupiter
Cooling System	Passively cooled to ~ 90 K
Attitude Control	3-axis controlled, 3 wheels, gyros, star trackers, sun sensors
Propulsion	Blow-down hydrazine with 8 thrusters
RF Communication	2 GHz transponders, 667 kbps down-link to 70 m DSN
Power	419 Watts
Mass	840 kg
Launch	Delta II 7425-10 on June 30, 2001 at 3:46:46.183 EDT
Orbit	1° - 10° Lissajous orbit about second Lagrange point, L2
Trajectory	3 Earth-Moon phasing loops, lunar gravity assist to L2
Design Lifetime	27 months = 3 month trajectory + 2 yrs at L2

[a] Commercial waveguide band designations used for the five *MAP* frequency bands
[b] Typical values for a radiometer are given.
[c] Effective signal bandwidth.
[d] The beam patterns are not Gaussian, and thus are not simply specified. The size given here is the square- root of the beam solid angle.
[e] Effective system temperature of the *entire system*.

Figure 6.4: WMAP specifications.[15]

Chapter 7

The Data

WMAP data can be found electronically by visiting *http://lambda.gsfc.nasa.gov*. I personally used the data specified as ´´Three-Year Data" and more specifically the ´´Full Resolution Coadded Three Year Sky Maps". For my analysis, I used maps that provided temperature data given for each differential assembly. Documentation about the data can be found in *M. Limon, et al*. Particularly, the temperature data for the differential assemblies comes in galactic coordinates and is given in units of mK. The 10 files contained there have a total number of 3,145,728 pixels. *Each pixel in a map represents a sky temperature for the bandpass appropriate to the differencing assembly.*[1]. The dipole described in chapter 3 has been removed from this data.

7.1 About HEALPix

HALPix[2] is an abbreviation for Hierarchical, Equal Area, and iso-Latitude Pixelisation of the sphere.[5]. HEALPix is very used in Cosmic Microwave Background Radiation applications because it is very useful to have maps in a discrete number of pixels including as much information as possible. HEALPix divides a spherical surface in pixels that cover the same area. Figure 7.1 show how HEALPix discretizes the sphere in different resolutions increasing from left to right. HEALPix is used in CMBR specially in the WMAP mission by receiving the data of the

[1]Wilkinson Microwave Anisotropy Probe (WMAP): Explanatory Supplement, editor M. Limon, et al (Greenbelt, MD: NASA/GSFC), pg. 37. Available in electronic form at http://lambda.gsfc.nasa.gov

[2]http://healpix.jpl.nasa.gov

full sky in resolutions of tenth of a degree making the sphere of the full sky to be divided in millions of pixels.

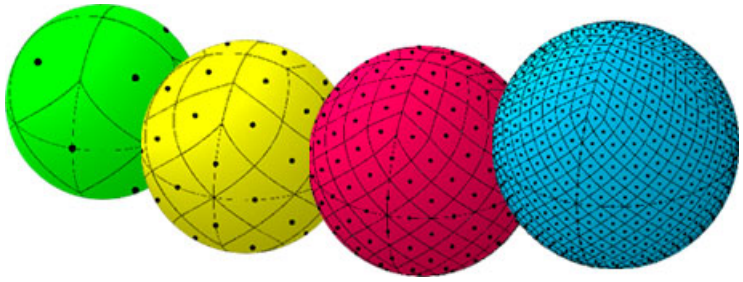

Figure 7.1: Pixelisation of the sphere made by HEALPix[14]

HEALPix makes the partition of the sphere by taking quadrilaterals which can have different shapes but they all have the same areas. The grid is said to have a resolution of N_{side}. The data used in the analysis presented on this project has an N_{side} value of 512 and it is said to have resolution 9.

A HEALPix software package has been released and it has a free license, and it can be downloaded from *http://healpix.jpl.nasa.gov/healpixSoftwareGetHealpix.shtml*. It consists on Fortran 90 and IDL routines. It includes some programs for simulations of the CMBR in which the most important applications for the purpose of this project have to do with the calculus of the power spectrum and spherical harmonic coefficients.

A bandlimited function is one whose fourier transform is zero after a certain finite frequency. In that case, the function f can be expanded in the spherical harmonics as shown by equation 7.1 in which γ gives the direction, Y_{lm} are the spherical harmonics.

$$f(\gamma) = \sum_{l=0}^{l_{max}} \sum_{m=-l_{max}}^{m=l_{max}} a_{lm} Y_{lm}(\gamma) \tag{7.1}$$

Appendix A shows how this is made for the power spectrum of the CMBR and shows what is the desired function f. What is important here, is the way in which HEALPix pixelizes it by calculating coefficient a_{lm} as shown in equation 7.2 by locating γ_p taking into account that $p \in [0, N_{pix} - 1]$. The superscript $*$ means complex conjugation is taken out.

$$f(\gamma) = \frac{4\pi}{N_{pix}} \sum_{p=0}^{N_{pix}-1} Y^*_{lm}(\gamma_p) f(\gamma_p) \tag{7.2}$$

7.2 FITS files

Data from WMAP published in NASA's webpage usually comes in a format extension .FITS. FITS is a very used format in astrophysics and it means "Flexible Image Transfer System". The file can contain images but it can also include information of data sets. The data comes in arrays which can be one, two, or three dimensional. NASA talks about this as 1-D spectra, 2-D images or tables with rows and columns of data, and 3-D data cubes. The FITS files also contain headers that are very useful for transmitting information about the contained data.

Data from each map for each differential assembly comes in a FITS file including two columns. The first column gives the thermodynamic temperature of each pixel given in mK. The second column gives an effective number of observations made by the WMAP for each pixel. A table for calculating pixel noise is given in Limon's WMAP supplement and shown in table 7.1. The noise for each pixel, given by σ, can be calculated as shown in equation 7.3.

Differential Assembly	σ_0 [mK]
K1	1.42366
Ka1	1.44883
Q1	2.26677
Q2	2.15567
V1	3.28789
V2	2.93683
W1	5.85196
W2	6.53276
W3	6.88032
W4	6.72537

Table 7.1: Coefficients to calculate pixel noise [31]

$$\sigma = \frac{\sigma_0}{\sqrt{N_{obs}}} \tag{7.3}$$

7.3 Choosing the Best Region of the Sky

As described in Bennet,et al, the WMAP probe has been measuring in five different frequencies to detect what is really microwave background and what is foreground emission. Foreground Masks have been made in order to filter pixels of the maps that have been contaminated with foreground emission. The foreground contamination has a dependence on the frequency being measured and having greater impact at lower frequencies. Due to this, the masks are created based on the K band frequency which is the smaller as shown in table 6.1.

The most important type of foreground emission received is the galactic microwave emission. This is a contamination received from the Milky Way, and it has three major causes: Free-free emission, Synchrotron emission, and Thermal Dust emission. The Free-free emission has its origin in electron-ion scattering. Bennet shows that the temperature received by the WMAP related to this goes as $T_{ff} \approx \nu^{-2}$ with ν being the frequency being measured. The Synchrotron emission, has its origin in the acceleration of electrons present in the cosmic rays when they go through a magnetic field. It comes basically by electrons caught in the magnetic fields left by supernovas and some others around the whole galaxy. The temperature detected by radiometers in the WMAP goes as $T_s \approx \nu^{\beta}$ with $-3.1 < \beta < -2.6$. The Thermal Dust emission, is a thermal radiation that has a thermal origin in the dust that is spread all around the galaxy, and the detected temperature goes as $T_d \approx \nu^{1.6}$. There is one important possible cause of contamination which has to do with the electric dipole emission when the dust particles spin, and with the magnetic dipole emission when there are some of this grains that are fluctuating thermally. Today, not much is known about this last type of possible emission contaminating the data. So the five frequencies are used to detect the different types of emission free-free, synchrotron, thermal dust, spinning and magnetic dust emission, and of course the CMBR. A graph made by NASA showing this behavior can be seen in figure 7.2.

With all this in mind, Bennet and his group were able to make some masks. Those masks can be found in NASA's webpage [15] in the link "Ancillary Data". Figure 7.3 shows some masks made in which the number following the letter p increases meaning that a more severe cut of the sky has been made; a higher temperature has been taken and more of the sky.

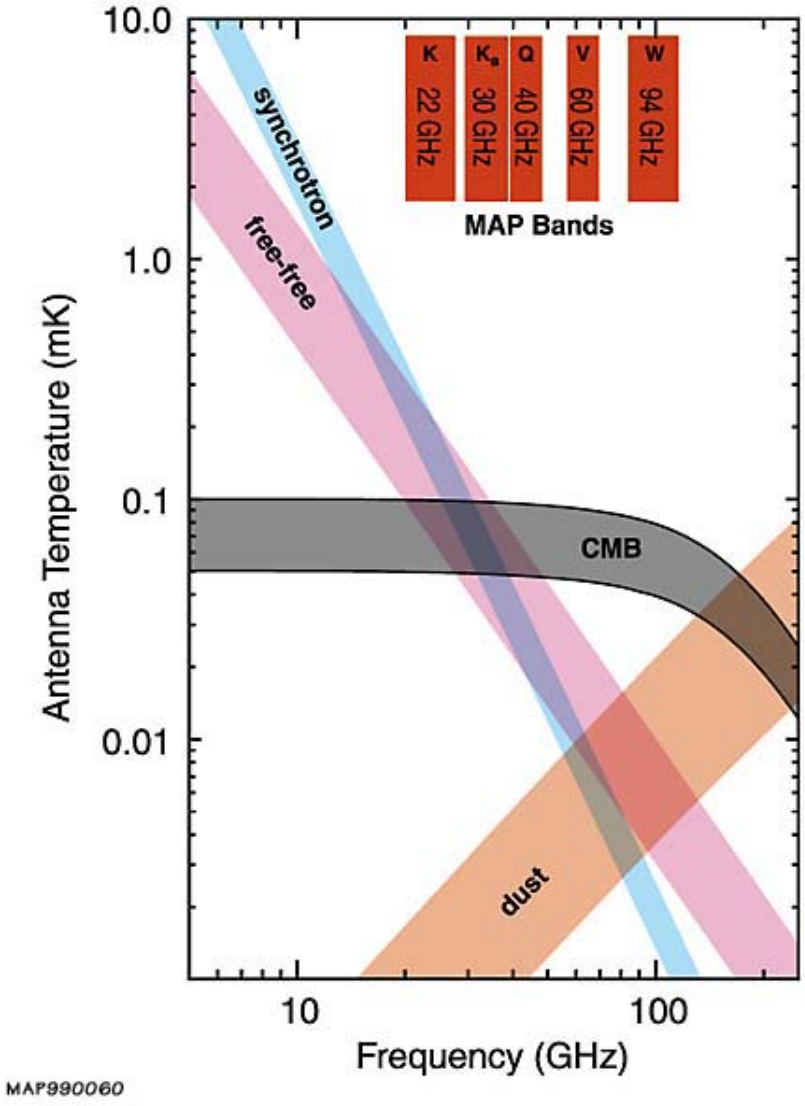

Figure 7.2: Behavior of the different sources of contamination generated by NASA and showing the bands of the WMAP and the CMBR. [20]

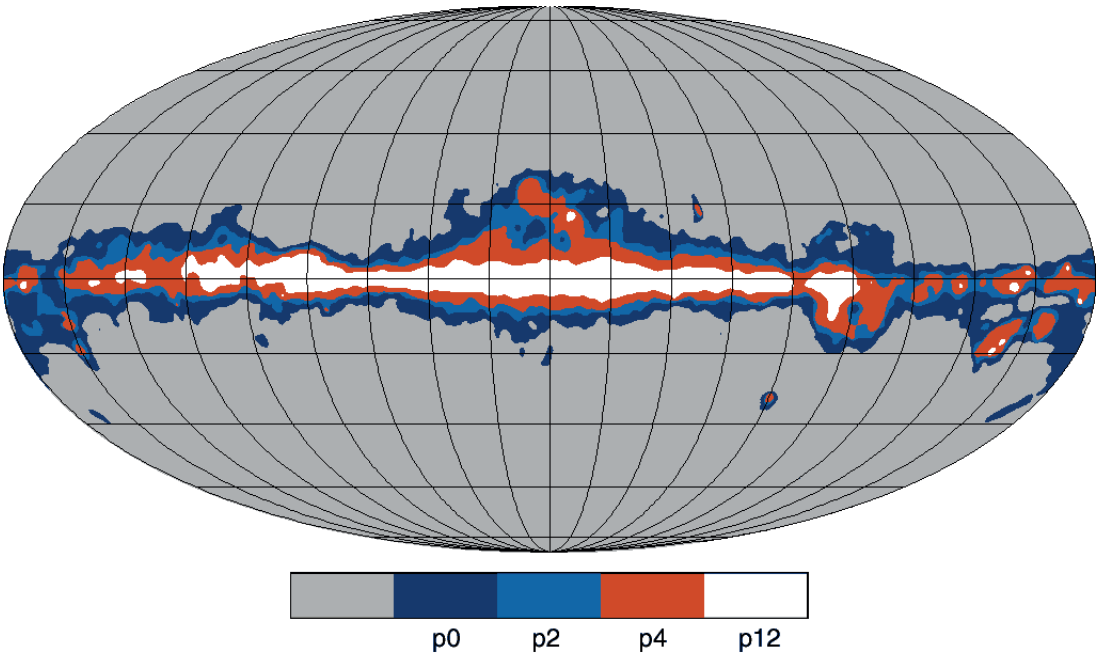

Figure 7.3: Masks for the CMBR made by Bennet and his team to make a cut of some pixels of the sky in order to have the least contamination as possible in the microwave region. [16]

Chapter 8

Processing the Data

8.1 The Test for Gaussianity

In many parts of this project I have mentioned that the CMBR has a Gaussian distribution. If the distribution was not Gaussian, then appendix A would be wrong and the calculus for the CMBR power spectrum should be ignored. When cosmologists talk about the Gaussianity of the CMBR, histograms become useful, and they are made counting pixels that have temperatures in certain ranges.

Figure 8.1 shows histograms for the 10 differential assemblies without using any mask to filter contamination. It can be seen that for higher frequencies, the graph is more symmetric and centered nearer the zero (because the average has been subtracted), while lower frequencies (K and Ka specially) are asymmetric at the right side. This shows the effect of the foreground emissions and how they depend on the different frequencies.

To subtract the noise or contamination due to foreground emission, I propose using a polynomial as shown in equation 8.1 which depends on the frequency and it has the spectral indices I talked about in the last chapter. In this case, I used a value of $\beta = -3$ for the synchrotron.

$$T(\nu) = a\nu^{-3} + b\nu^{-2} + c\nu^{-1} + d + e\nu^{1.6} \tag{8.1}$$

The temperature of each pixel without the foreground emission should then be given by equation 8.2.

$$T(\nu) = c\nu^{-1} + d \tag{8.2}$$

However, to find the coefficients a, b, c, d, e five equations are needed, but I have ten differential assemblies to choose. To solve this, I use another package of data found on the WMAP webpage, in which the data is presented with the same resolution and units as the differential assemblies, but using a weighted mean method a map for each frequency has been done obtaining five in total. Using this five maps, the different Histograms are shown in figure 8.2.

It can be seen that the graphs are more symmetric with respect to 0 making them to look more Gaussian around the average temperature of the CMBR. It can also be seen that specially in the K band, the foreground emission was reduced in great part, and the enlargement to the right has been eliminated. As frequency is increased, the Gaussian distribution is more thin. It can be clearly seen then that the procedure shown in appendix A is valid for the treatment of the calculus for the power spectrum of the CMBR.

8.2 The Power Spectrum

Knowing that the procedure from Appendix A works, the next step is calculating the c_l coefficients for the different differential assemblies. Here is where HEALPix turns to be very important. HEALPix contains some facilities that can be used for different purposes. One of those facilities is called $anafast$ which I used to calculate the a_{lm} coefficients of the different differential assemblies maps. First, $anafast$ asks if the map is a temperature only map or if it contains information about polarization. For the purpose of this project, only temperature maps are used. $anafast$ can be used in double precision or single precision modes of $FORTRAN$. I used the double precision mode to do it. The next step is to tell the facility where is the $.FITS$ file containing the map temperature information located. The maximum value of l for the different calculations can also be established but it is recommended to use $l = 2N_{side}$ that for this case would be 1024. A mask can also be used and the file containing the mask should be specified. I used the $Kp2$ mask, and what $anafast$ actually does is that before making any calculation it multiplies each pixel's temperature by a value contained in the mask, subtracting some of the contamination found on it. A symmetric cut around the equator can be made specifying a latitude angle and specifying a zone which pixels will not be taken into account. I didn't make any cut and took all the pixels

of the files in my calculations. The next option is to choose between taking the dipole and the monopole from the data or use it as it is contained in the file. As the dipole and monopole have already been removed from the data provided by NASA, no dipole removal has been made. One can also specify the use of ring weight corrected quadrature which is also included in HEALPix, increasing accuracy. Finally, a number of iterations can be specified too in which a third order iteration is recommended. c_l an a_{lm} coefficients are saved on some output files which names are specified by the user too.

In appendix A, a rigorous demonstration has been made to show that the power spectrum coefficients C_l are given by equation 8.3.

$$C_l = a_l^2 \equiv \frac{1}{2l+1} \sum_{m=-l}^{l} |a_{lm}|^2 = \left\langle |a_{lm}|^2 \right\rangle \tag{8.3}$$

The next step is to calculate the c_l coefficients in a special way proposed by Hinshaw, et al. They propose a quadratic estimator in which the a_{lm} coefficients are given by equation 8.4. The ring weight W is applied by $anafast$ and an angle Ω_p is assumed to be covered by each pixel. The value ΔT is the one that comes in the FITS file from WMAP. p indicates the pixel number and the integral, which includes certain directions $\vec{n}$, is changed by a discrete sum over all the pixels shown in equation 8.5.

$$a_{lm} = \int d\Omega \Delta T(\vec{n}) W(\vec{n}) Y^*_{lm}(\vec{n}) \tag{8.4}$$

$$a_{lm} = \Omega_p \sum_p \Delta T(p) W(p) Y^*_{lm}(p) \tag{8.5}$$

$anafast$ calls one of the subroutines included in HEALPix called $map2alm$ which is the one encharged of reading the information from the file and calculating the a_{lm} coefficients. With the specification of the ring weights, the a_{lm} file obtained when running $anafast$ is precisely the value of the coefficient given by equation 8.5.

The important thing about Hinshaw's job, is the definition of the Cross Power Spectrum in which the coefficients c_l are given by equation 8.6. Coefficients a^i_{lm} and a^j_{lm} are the coefficients from the file, but for differential assemblies i and j respectively. The idea of doing this is that the noise from maps of different

differential assemblies has no correlation. As in an earlier occasion, the superscript $*$ represents complex conjugate. The frequency to take into account for this case is defined bye Hinshaw and his team as an effective frequency given by $\nu_{eff} = \sqrt{\nu_i \nu_j}$ where the subindexes indicate the differential assembly i and j respectively.

$$c_l = \frac{1}{2l+1} \sum_{m=-l}^{l} a_{lm}^{i} a_{lm}^{j*} \tag{8.6}$$

Equation 8.6 is of course very similar to 8.3 with the mentioned change of crossing the different differential assemblies.

Using the software *Fv* which has a free license and can be obtained from *http://heasarc.gsfc.nasa.gov/lheasoft/ftools/fv/*, the FITS files including the a_{lm} calculated with HEALPix facility is transformed to a file with the $.txt$ extension. A program made using *Wolfram Mathematica* is encharged of reading this new file and calculating the C_l coefficients for the Cross power spectrum. First of all it is important to understand how HEALPix releases the file. These a_{lm} file contains three columns labeled index, real, and imaginary respectively. The first column gives the information about the l and m because the index is given using the equation 8.7. The second and third columns give the real and imaginary parts of the a_{lm} coefficients respectively.

$$Index = l^2 + l + m + 1 \tag{8.7}$$

Appendix C shows the Mathematica algorithm used for making this. It basically works by reading the $.txt$ file and writing the $C_l's$ on another output file. The K and Ka differential assemblies are not used due to their high noise level so a total of 28 files are obtained for the combination of the other 8 differential assemblies files.

As shown in Appendix A, the function to graph in order to gather information is the one shown in equation 8.8. In this case, I am particularly interested on seeing how does the function changes as l changes. The obtained graph is shown in figure 8.3.

$$\frac{\Delta T}{\langle T \rangle} = \left(\frac{l(l+1)}{2\pi} C_l \right) \tag{8.8}$$

8.3 Extracting Important Information

Now that the power spectrum has been made, the next step is to take as much information as possible from it. I will begin from equation 8.9 that comes out from the definition of the density parameter Ω.

$$\frac{H^2\Omega}{(1+z)^3} = constant = \Omega_0 H_0^2 \tag{8.9}$$

It is also important to know about the angular diameter distance. This gives information about how far an object appears to be assuming Euclidean geometry and knowing the physical extent of it which is represented as x. It then follows equation 8.10. $Sin\theta$ has been approximated to θ because in astronomy, this angle is very small due to the large distance between objects in the universe.

$$d_{diam} = \frac{l}{Sin\theta} \approx \frac{l}{\theta} \tag{8.10}$$

Assuming the observer is in the origin and the object is at r_0, the physical extent of it is $x = r_0 a(t_e) d\theta$ where the scale factor has been added at the time t_e when the light was emitted by the object. The angle $d\theta$ is then $\frac{x}{r_0 a(t_e)}$ or if it is written in terms of the present scale factor a term involving the redshift appears and the result can be expressed as $\frac{x(1+z)}{r_0 a_0}$. Replacing in equation 8.10 the expression shown in equation 8.11 is obtained.

$$d_{diam} = \frac{a_0 r_0}{1+z} \tag{8.11}$$

Eventhough I will not show it here, when $z >> 1$ $a_0 r_0$ can be approximated as shown in equation 8.12.

$$a_0 r_0 \approx \frac{2c}{H_0\sqrt{\Omega_0}} \tag{8.12}$$

This can now be used to determine the angle covered by a certain Hubble length at time of decoupling; time which we have the information of the CMBR. To do this, equation 8.11 is used and replacing equation 8.13 is obtained. The distance x in terms of the Hubble parameter is $\frac{c}{H}$ canceling it in the result.

$$\theta = \frac{x(1+z)}{a_0 r_0} = \frac{x(1+z)H_0\sqrt{\Omega_0}}{2c} = \frac{x(1+z)H_0 H\sqrt{\Omega}}{2c(1+z)^{\frac{3}{2}}H_0} = \frac{\sqrt{\Omega}}{2\sqrt{1+z}} \tag{8.13}$$

The angle θ can be determined from the Power Spectrum of figure 8.3 as the scale is approximately $\theta = \frac{180^\circ}{l}$ so it is useful to calculate Ω which will be the density parameter at the time of decoupling. A graph showing how θ changes in function of Ω is shown in figure 8.4. Eventhough equation 8.13 gives the angle in radians, the graph shows it in degrees after the conversion has been made. The value of z has been taken to be 1000 as it is its approximate value in the time of decoupling.

The last procedure is valid when taking a flat cosmology which includes a cosmological constant. The next thing I will show is the same situation for an open universe with no cosmological constant. In this case, the angular diameter distance is given by equation 8.14.

$$d_{diam} = \frac{2c}{H_0} \frac{\Omega_0 z + (\Omega_0 - 2)(\sqrt{1 + \Omega_0 z} - 1)}{\Omega_0^2 (1 + z)^2} \tag{8.14}$$

Using the fact that $z >> 1$ at least for the desired situation which is decoupling, equation 8.14 can be approximated to equation 8.15.

$$d_{diam} \approx \frac{2c}{H_0} \frac{z\Omega_0}{\Omega_0^2 z^2} = \frac{2c}{H_0} \frac{1}{\Omega_0 z} \tag{8.15}$$

To find theta it is just necessary to make the procedure shown in equation 8.16 in which equation 8.9 has been used to replace $\frac{H_0}{H}$.

$$\theta = \frac{cH^{-1}}{d} = \frac{H_0}{H} \frac{\Omega_0 z}{2} = \frac{\sqrt{\Omega}}{\Omega_0 (1 + z)^3} \frac{\Omega_0 z}{2} \approx \frac{1}{2} \sqrt{\frac{\Omega \Omega_0}{z}} \tag{8.16}$$

In chapter 5 I showed that Ω is very close to 1 so making this assumption the angle covered by a certain object is then finally shown in equation 8.17.

$$\theta \approx \frac{1}{2} \sqrt{\frac{\Omega_0}{z}} \tag{8.17}$$

Taking the value for z at decoupling another graph of the angle vs. Ω_0 can be made and it is shown in figure 8.5.

The graph of the power spectrum shows a maximum for all the 28 combinations of the differential assemblies at $l \approx 220$. This covers an angle of approximately $\theta = \frac{180_\circ}{220} \approx 0.82^\circ$. This means that most of the structures in decoupling covered an angle of 0.82°. Taking a look at figure 8.4 it can be noticed that this

angle corresponds to an Ω very close to one. The same thing can be seen from figure 8.5 in which Ω_0 has a value very close to unity too.

Throughout the project I have been saying and showing that from the Friedmann equation $\Omega \approx 1$ would say that the universe has a flat geometry. The CMBR power spectrum lets us confirm that we live in a flat universe in which the angles of a triangle add up to 180° and the circumference of a circle is given by $2\pi r$. This flat universe has been flat at decoupling and in the present.

Another very important thing that can then be seen is that the power spectrum obtained seems to confirm or at least give a very important validity to Inflation. I showed that inflation predicts a flat universe in which this geometry is conserved in time, and that is exactly what the power spectrum is showing.

Chapter 5 shows information about different $\Omega's$ we are able to measure. However adding all those $\Omega's$ the obtained value is far away from one. Dark matter is what we suppose is encharged of adding the rest and it is what conforms the great majority of the universe. I will not enter a discussion about this and just wanted to mention it.

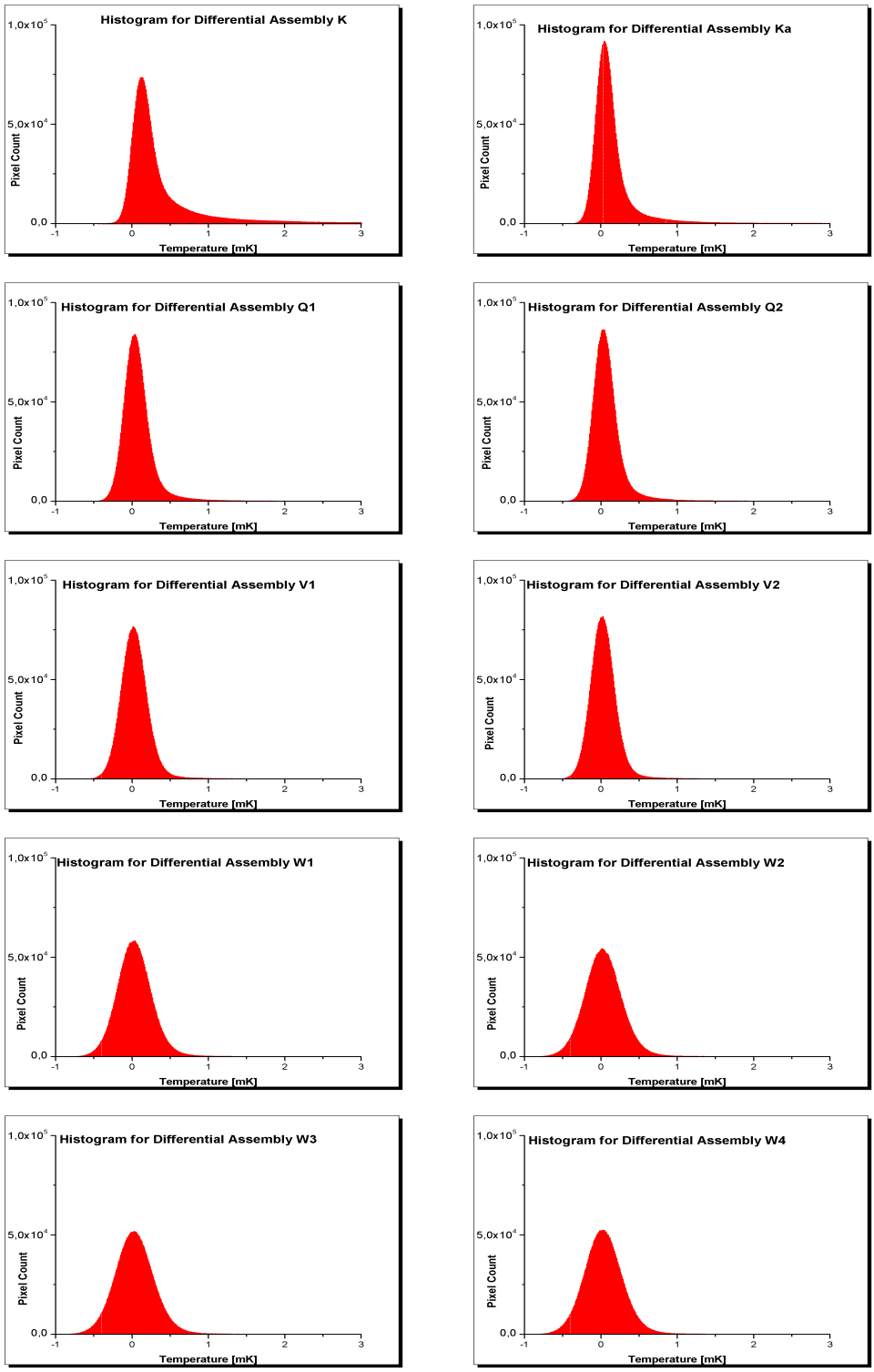

Figure 8.1: Histograms for the differential assemblies

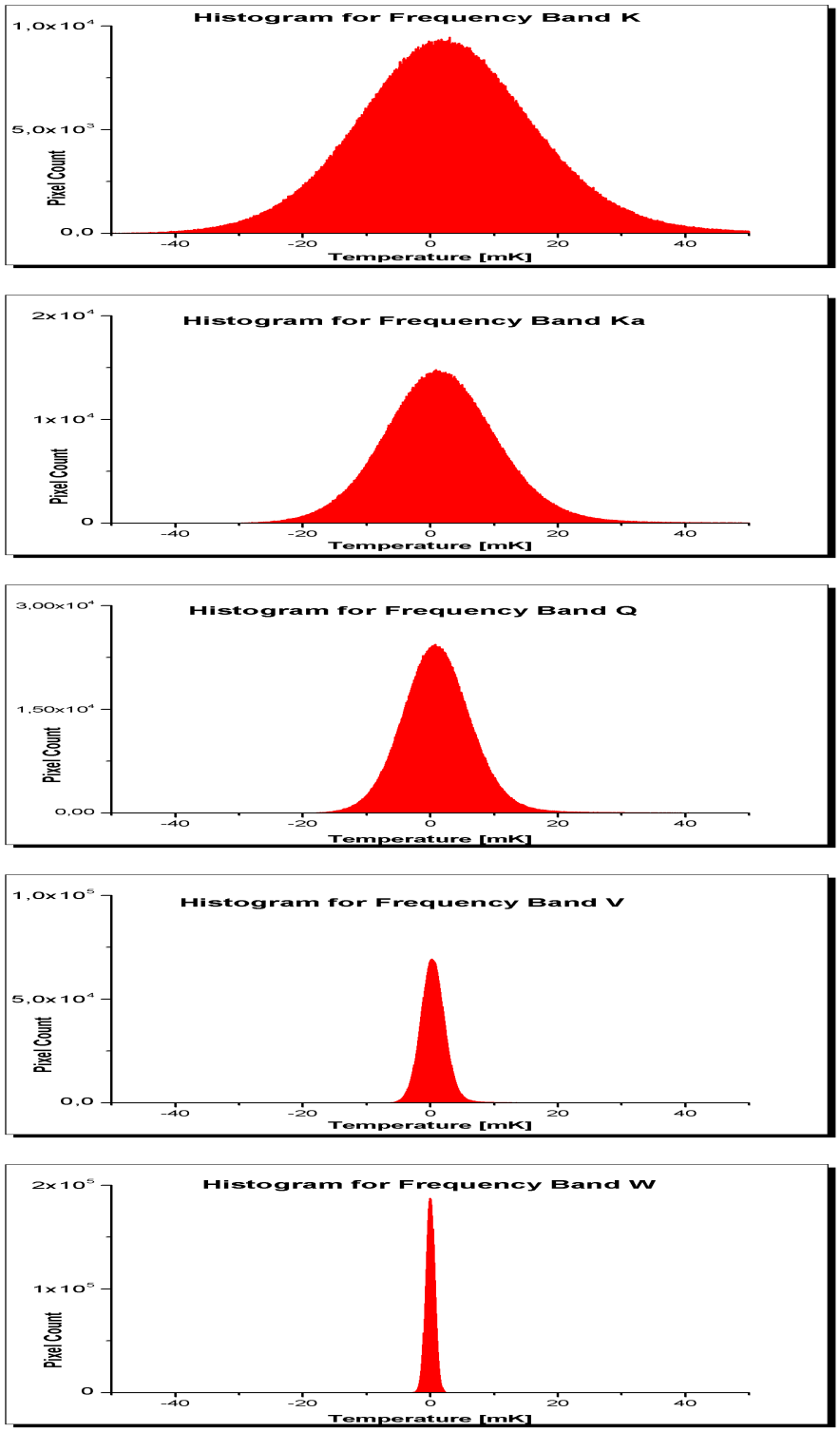

Figure 8.2: Histograms for the different frequency bands.

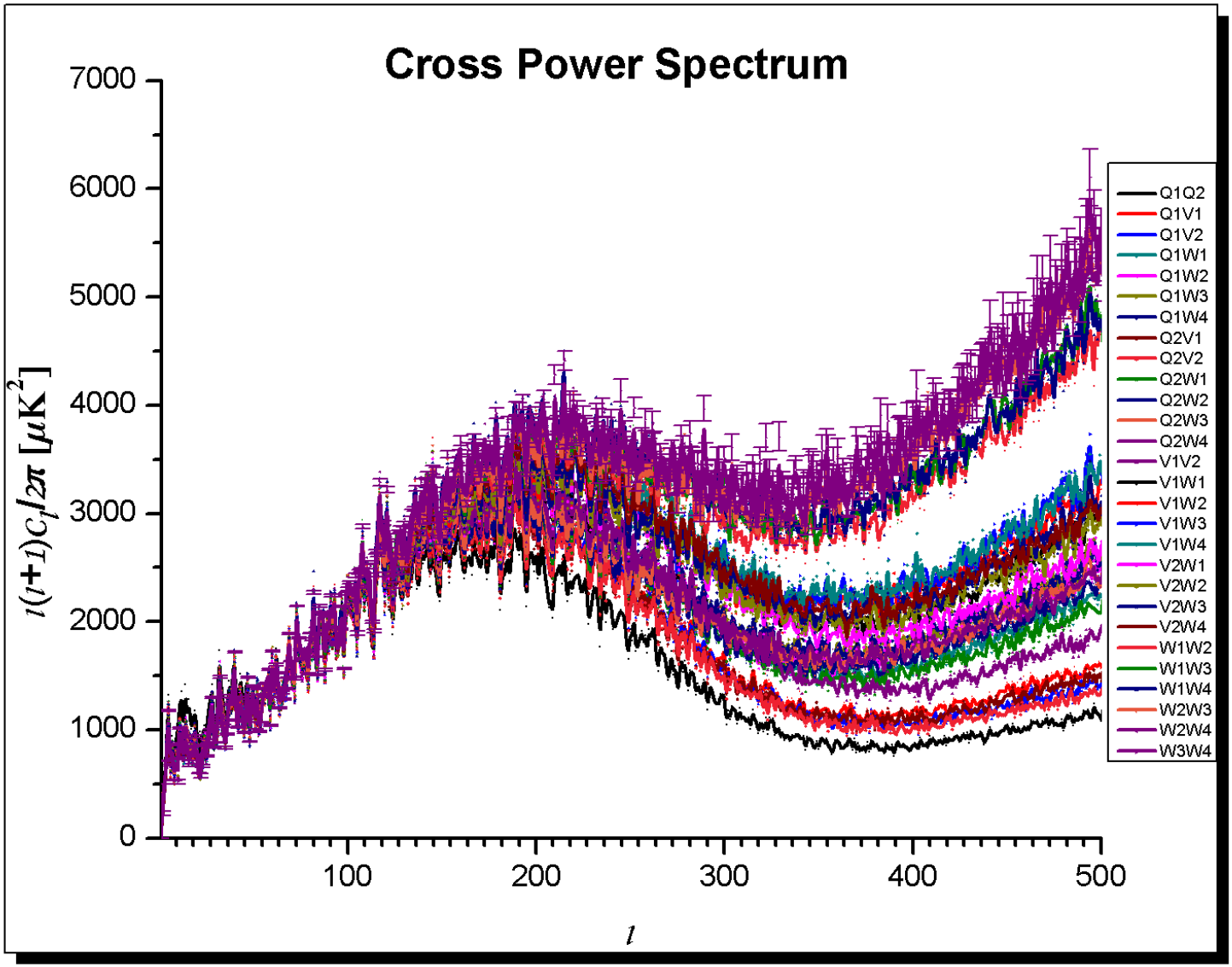

Figure 8.3: Cross power spectrum made for the 28 combinations of the 8 differential assemblies excluding K and Ka. The function $l(l+1)C_l/2\pi$ has been graphed in function of the multipolar moment l.

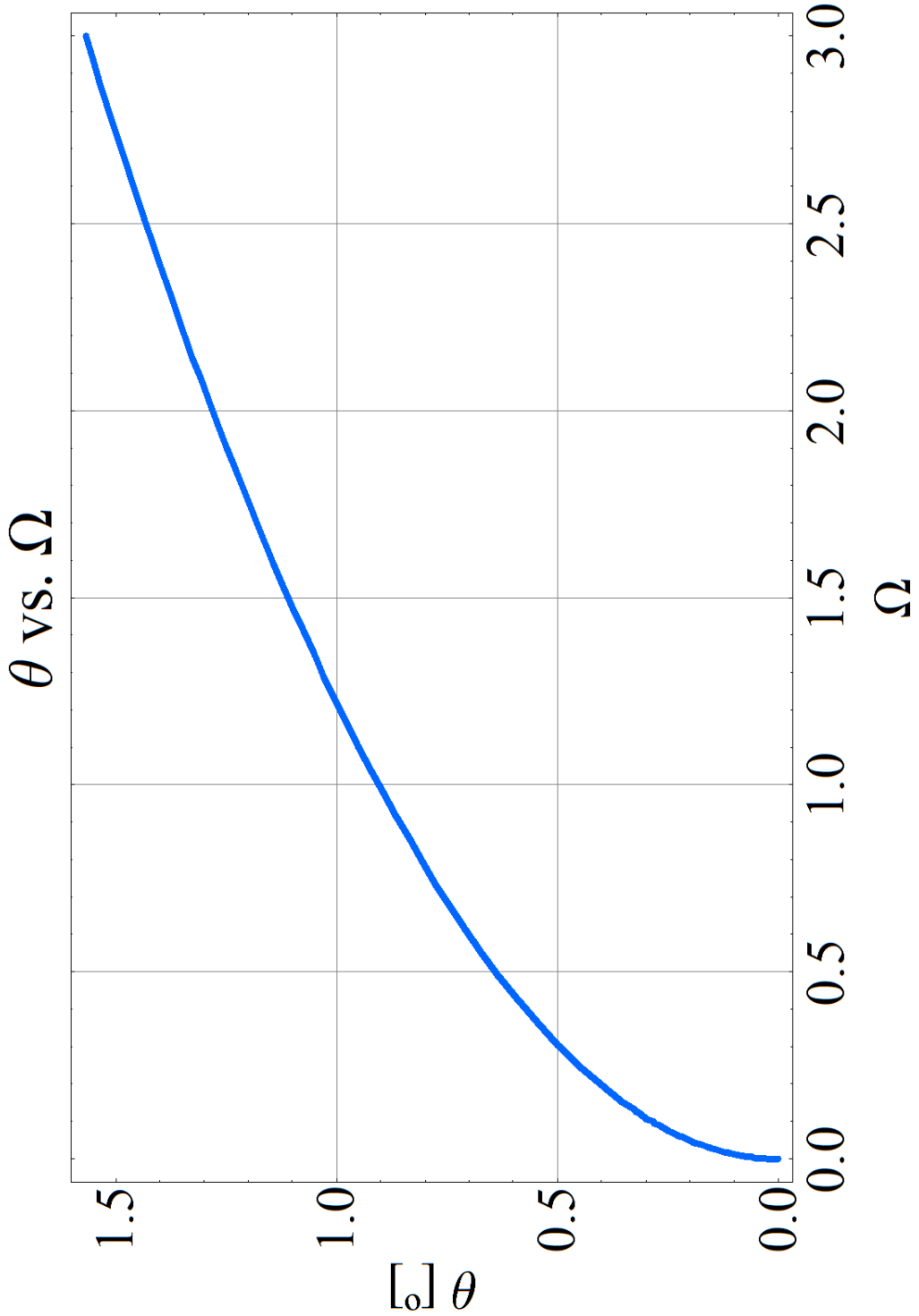

Figure 8.4: θ as a function of Ω in which the procedure for doing it is valid for a flat cosmology with a cosmological constant.

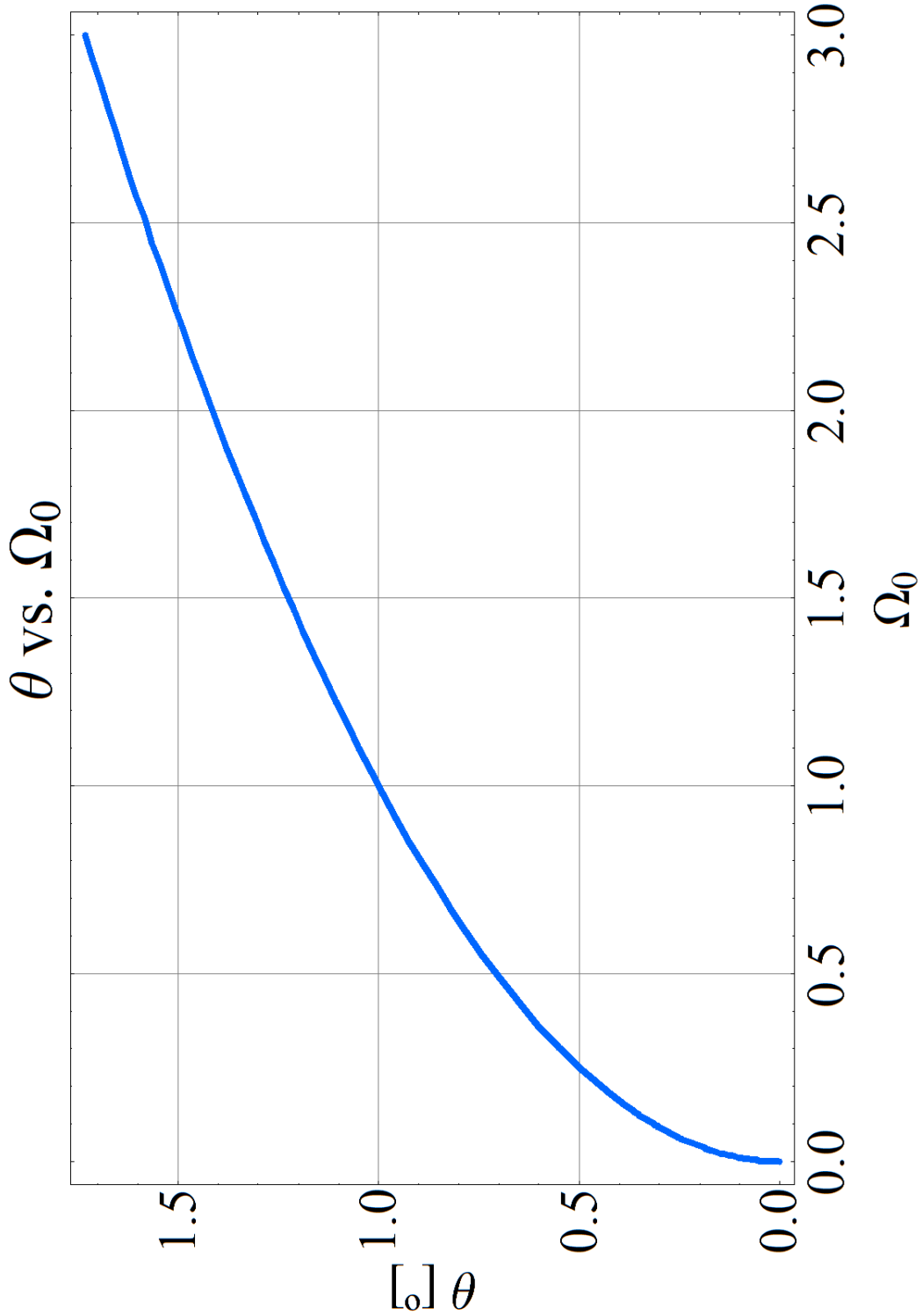

Figure 8.5: θ as a function of Ω in which the procedure for doing it is valid for an open universe with no cosmological constant.

Chapter 9

Conclusions

I began this project with a brief description of the history of our Universe as we think it is. Then, I talked about Cosmology in which using the Friedmann Equation we can get information about the geometry of the Universe. Writing it in terms of the Hubble Parameter H, and introducing a cosmological constant Λ are things done in that part of the project. In the next step, a description of the Cosmic Microwave Background Radiation and some information about its origin was made. The Dipole anisotropy due to Earth's Kinematics was explained followed by a very brief description of what is said to be the intrinsic anisotropies on it. To give an end to this first part full of theoretical information, I mentioned Inflation as a theory to help solve some inconsistencies in what we were saying about the Big Bang.

A second part of the project was made and talked about collecting data about the Cosmic Microwave Background Radiation which is the primary topic of this project. A description of NASA's WMAP mission was made, and data collected by this very important space probe was gathered. It was needed to use some special software for the processing and reading of the different files in which temperature for different pixels (the sky was made discrete) of the sky was desired for the analysis. I then proposed a way of taking out the microwave contamination, or that it has its origin in a different source than decoupling, to test the Gaussian distribution of the anisotropies in the CMBR. They evidently seemed to justify the procedure exposed in detail in Appendix A.

Finally and the most important part of this project, I showed a way of calculating the Power Spectrum for the CMBR in which a cross-power is used. A

graph gave information about the angular extension of structures in the time of decoupling in which it was shown they were mostly of about 1°. With this, I got to the conclusion that our Universe is and has been flat, and certain validation for the idea of inflation was given. An open discussion was left about the constituents of our universe which seem to be a very great percentage of what we call dark matter.

Appendix A

Spherical Harmonics Decomposition for the CMBR.

When a quantity is defined over a spherical surface, in this case the surface of last scattering, in which the desired quantity is $\frac{\Delta T}{T}$, is useful to make a decomposition in spherical harmonics. Equation A.1 shows how it is done for this case in which $\hat{q}$ is a desired direction and Y_{lm} are the spherical harmonics.

$$\frac{\Delta T}{T}(\hat{q}) = \sum_{l=1}^{\infty} \sum_{m=-l}^{m=l} a_{lm} Y_{lm}(\hat{q}) \tag{A.1}$$

The coefficients a_{lm} represent the power of the Y_{lm} and are given by equation A.2.

$$a_{lm} = \int d\Omega \frac{\Delta T}{T}(\hat{q}) Y_{lm}(\hat{q}) \tag{A.2}$$

Spherical Harmonics are defined in such a way that they satisfy the normalization equation A.3 in which the δ symbol represents the Kronecker delta, and the integral is taken out along the entire sphere.

$$\int d\Omega Y_{lm} Y_{l'm'} = \delta_{ll'} \delta_{mm'} \tag{A.3}$$

The summation theorem seen in equation A.4 lets us see that all the statistical information of $\frac{\Delta T}{T}$ is perfectly described by the coefficients a_{lm}. In this equation,α represents the angle between two chosen directions $\hat{q}$ and $\hat{p}$,and P_l are the Legendre Polynomials.

$$\sum_m Y_{lm}(\hat{p})Y_{lm}(\hat{q}) = \frac{2l+1}{4\pi}P_l(Cos(\alpha)) \tag{A.4}$$

When talking about CMBR, usually the term l=1 is not included in the summation because this dipole term has a bigger value compared with others and its origin is mostly kinematic.

Cosmologists are mostly interested in a statistical property of $\frac{\Delta T}{T}$ called the correlation function $C(\theta)$. Two points on the surface of last scattering are chosen and they are localized in directions $\hat{q_1}$ and $\hat{q_2}$ with an angular separation θ given by $Cos(\theta) = \hat{q_1} \cdot \hat{q_2}$. So to find the value of the correlation function it is necessary to multiply the values of $\frac{\Delta T}{T}$ in both points and take the average over all the points separated by an angle θ as shown in equation A.5.

$$C(\theta) = \left\langle \frac{\Delta T}{T}(\hat{q_1})\frac{\Delta T}{T}(\hat{q_2}) \right\rangle \tag{A.5}$$

The correlation function will then be calculated explicitly as shown in equation A.6 and where equation A.1 has been used.

$$C(\theta) = \sum_{l=1}^{\infty}\sum_{m=-l}^{l} a_{lm}^2 Y_{lm}(\hat{q_1})Y_{lm}(\hat{q_2}) \tag{A.6}$$

Using equation A.4 equation A.6 can be rewritten as seen in equation A.7.

$$C(\theta) = \sum_{l=1}^{\infty} a_{lm}^2 \frac{(2l+1)}{4\pi}P_l(Cos(\theta)) \tag{A.7}$$

For Gaussian statistics, coefficients a_{lm} have random phases but are independent for each mode l. It is convenient to define a relative coefficient C_l for each of these modes as shown in equation A.8.

$$C_l = a_l^2 \equiv \frac{1}{2l+1}\sum_{m=-l}^{l} |a_{lm}|^2 = \left\langle |a_{lm}|^2 \right\rangle \tag{A.8}$$

Finally the correlation function can be expressed as shown in equation A.9.

$$C(\theta) = \frac{1}{4\pi}\sum_{l=1}^{\infty}(2l+1)C_l P_l(Cos(\theta)) \tag{A.9}$$

A measurement of $C(\theta)$ can be used to find the multipolar moments C_l. This moments will be different from zero for angular scales greater than the resolution of the experimental instrument, and smaller than the piece of sky being examined. C_l gives a measurement of temperature fluctuations at a scale in which $\theta \approx 180/l$. If the mean temperature has been well established then the monopole term vanishes. The dipole term in which l=1, comes mostly from doppler shift due to earth kinematics. Terms in which $l \geq 2$ are the ones of interest in the CMBR analysis because they have the information of fluctuations occurring in the time of last scattering.

The angular spectrum is then calculated as shown in equation A.10

$$C_l = \int_{-l}^{l} d\mu C[y(\mu)] P_l(\mu) \tag{A.10}$$

$$y(\mu) \equiv \int Cosh(\mu) - \mu Sinh(\mu) \tag{A.11}$$

Experimental data is usually presented by graphing the function of equation A.12 in which the contribution per logarithmic interval to total temperature fluctuation ΔT of the CMBR is gathered.

$$\Delta T = \left(\frac{l(l+1)}{2\pi} C_l \right) \langle T \rangle \tag{A.12}$$

Appendix B

Demonstrations of useful equations

B.1 The Friedmann Equation

Here a demonstration of the Friedmann equation is going to be made without using General Relativity. Instead I will use the Newtonian Gravity which will lead to the same result.

The Newtonian law of gravity says that the force acting on an object of mass m and produced by another one of mass M which are separated by a distance r follows equation B.1. G is the gravitational constant and whose value is $6.673 \times 10^{-11} Nm^2/Kg^2$

$$F = \frac{GMm}{r^2} \tag{B.1}$$

This force generates a gravitational potential V shown in equation B.2.

$$V = -\frac{GMm}{r} \tag{B.2}$$

Taking into account a mass M with mass density ρ and a test particle (small mass not necessarily punctual mass) then equation B.3 must be valid for a spherical distribution of mass. It doesn't really matter the shape as the force exerted only depends of the total mass located in the center of mass of the material. Equation B.1 can then be rewritten as shown in equation B.4.

$$M = \frac{4\pi\rho r^3}{3} \tag{B.3}$$

$$F = \frac{4\pi G\rho r m}{3} \tag{B.4}$$

The potential energy of the testing particle is then expressed in terms of ρ as shown in equation B.5.

$$V = -\frac{4\pi G\rho r^2 m}{3} \tag{B.5}$$

The testing particle has a kinetic energy T as shown in equation B.6. The velocity of the particle is $\frac{dr}{dt} = \dot{r}$

$$T = \frac{1}{2}m\dot{r}^2 \tag{B.6}$$

Using the conservation of energy in which the total energy is $U = T + V$, equation B.7 is obtained.

$$U = \frac{1}{2}m\dot{r}^2 - \frac{4\pi G\rho r^2 m}{3} \tag{B.7}$$

Using the comoving coordinate system described in chapter 2, $\vec{r} = a(t)\vec{x}$ with a being the scale factor, the total energy equation can be rewritten as shown in equation B.8.

$$U = \frac{1}{2}m\dot{a}^2 x^2 - \frac{4\pi G\rho a^2 x^2 m}{3} \tag{B.8}$$

If both sides are multiplied by $\frac{2}{ma^2x^2}$ equation B.9

$$U\frac{2}{ma^2x^2} = \left(\frac{\dot{a}}{a}\right)^2 - \frac{8\pi G\rho}{3} \tag{B.9}$$

Defining $kc^2 \equiv -\frac{2U}{mx^2}$ and rearranging terms, equation B.10 is written which is precisely the Friedmann equation.

$$\left(\frac{\dot{a}}{a}\right)^2 = \frac{8\pi G\rho}{3} - \frac{kc^2}{a^2} \tag{B.10}$$

B.2 The Fluid Equation

To demonstrate this equation, the first law of thermodynamics is needed. The relation shown in equation B.11 describes a change in energy E relating the pressure p with a change in the volume V and the temperature T including a change in entropy S. The first law is applied to a volume that has a comoving radius.

$$dE + pdV = TdS \tag{B.11}$$

The energy is $E = mc^2$ so it can be written as shown in equation B.12.

$$E = \frac{4\pi}{3}a^3\rho c^2 \tag{B.12}$$

Using the chain rule equations B.13 and B.14 are obtained showing how the energy and the volume change with time.

$$\frac{dE}{dt} = \frac{4\pi}{3}a^3\frac{d\rho}{dt}c^2 + 4\pi a^2\rho c^2\frac{da}{dt} \tag{B.13}$$

$$\frac{dV}{dt} = 4\pi a^2\frac{da}{dt} \tag{B.14}$$

If the expansion is reversible, then $ds = 0$, and replacing the last two expressions in the first law of thermodynamics then the equation B.15 is obtained.

$$\frac{4\pi}{3}a^3\dot{\rho}c^2 + 4\pi a^2\rho c^2\dot{a} + p4\pi a^2\dot{a} = 0 \tag{B.15}$$

Dividing all the equation by $\frac{4\pi}{3}a^3c^2$ and factoring $3\frac{\dot{a}}{a}$ in the last two terms then the fluid equation shown in equation B.16 is obtained.

$$\dot{\rho} + 3\frac{\dot{a}}{a}\left(\rho + \frac{p}{c^2}\right) = 0 \tag{B.16}$$

B.3 The Acceleration Equation

The acceleration equation is very simple to proof having the Friedmann and the Fluid equations. The first thing to do is to take the derivative of the Friedmann equation with respect to time obtaining equation B.17.

$$2\frac{\dot{a}}{a}\frac{a\ddot{a} - \dot{a}^2}{a^2} = \frac{8\pi G}{3}\dot{\rho} + 2\frac{kc^2\dot{a}}{a^3} \tag{B.17}$$

From equation B.17 $\dot{\rho}$ can be taken and inserted in the Fluid equation. After rearranging terms the equation shown in B.18 is obtained.

$$\frac{\ddot{a}}{a} - \left(\frac{\dot{a}}{a}\right)^2 = -4\pi G\left(\rho + \frac{p}{c^2}\right) + \frac{kc^2}{a^2} \tag{B.18}$$

Replacing the term $\left(\frac{\dot{a}}{a}\right)^2$ using the Friedmann equation, the acceleration equation is obtained as shown in equation B.19.

$$\frac{\ddot{a}}{a} = -\frac{4\pi G}{3}\left(\rho + \frac{3p}{c^2}\right) \tag{B.19}$$

Appendix C

Algorithms for the Calculus of the Power Spectrum

I show here some algorithms used for the calculus of the power spectrum. The algorithms are made using the programming language of *Wolfram Mathematica*.

C.1 Remove Foreground Contamination

The next algorithm shows a program that reads the temperature data for each pixel and for each frequency band, and removes the noise as described in section 8.1.

```
K1 = OpenWrite["Route to folder\K1.txt"];
Ka1 = OpenWrite["Route to folder\Ka1.txt"];
Q1 = OpenWrite["Route to folder\Q.txt"];
V1 = OpenWrite["Route to folder\V.txt"];
W1 = OpenWrite["Route to folder\W.txt"];
K1dat = OpenRead[
 "Route to folder\wmap_band_imap_r9_3yr_K_v2_t1.txt"];
Ka1dat = OpenRead[
 "Route to folder\wmap_band_imap_r9_3yr_Ka_v2_t1.txt"];
Q2dat = OpenRead[
 "Route to folder\wmap_band_imap_r9_3yr_Q_v2_t1.txt"];
V1dat = OpenRead[
 "Route to folder\wmap_band_imap_r9_3yr_V_v2_t1.txt"];
W1dat = OpenRead[
```

```
 "Route to folder\wmap_band_imap_r9_3yr_W_v2_t1.txt"];
f1:=23 * 10^9
f2:=33 * 10^9
f3:=41 * 10^9
f4:=61 * 10^9
f5:=94 * 10^9
For[i = 1, i<=3145728, i++,
 ar1 = Read[K1dat, {Real, Real, Real}];
ar2 = Read[Ka1dat, {Real, Real, Real}];
ar3 = Read[Q2dat, {Real, Real, Real}];
ar4 = Read[V1dat, {Real, Real, Real}];
ar5 = Read[W1dat, {Real, Real, Real}];

coeficientes = Solve [{ar1[[1]]==a f1^-3 + b f1^-2 + c f1^-1 + d + e f1^1.6,
ar2[[1]]== a f2^-3 + b f2^-2 + c f2^-1 + d + e f2^1.6,
ar3[[1]]== a f3^-3 + b f3^-2 + c f3^-1 + d + e f3^1.6,
ar4[[1]]==a f4^-3 + b f4^-2 + c f4^-1 + d + e f4^1.6,
 ar5[[1]]==a f5^-3 + b f5^-2 + c f5^-1 + d + e f5^1.6}, {a, b, c, d, e}];
 tercero = c/.coeficientes;
cuarto = d/.coeficientes;
 Write [K1, {i, tercero f1^-1 + cuarto}];
Write [Ka1, {i, tercerof2^-1 + cuarto}];
Write [Q1, {i, tercerof3^-1 + cuarto}];
Write [V1, {i, tercerof4^-1 + cuarto}];
Write [V2, {i, tercerof4^-1 + cuarto}];
Write [W1, {i, tercerof5^-1 + cuarto}];

]
```

C.2 Cross Power Spectrum

The next algorithm shows a program that reads the a_{lm} coefficients for each differential assembly, and calculates the C_l coefficients for the cross power spectrum. It reads 8 files and returns 28 files for all the possible combinations of the differential assemblies. Details are shown in chapter 8.

```
archivo1 = OpenWrite["Route to folder\q1_q2.txt"];
archivo2 = OpenWrite["Route to folder\q1_v1.txt"];
archivo3 = OpenWrite["Route to folder\q1_v2.txt"];
archivo4 = OpenWrite["Route to folder\q1_w1.txt"];
archivo5 = OpenWrite["Route to folder\q1_w2.txt"];
archivo6 = OpenWrite["Route to folder\q1_w3.txt"];
archivo7 = OpenWrite["Route to folder\q1_w4.txt"];
archivo8 = OpenWrite["Route to folder\q2_v1.txt"];
archivo9 = OpenWrite["Route to folder\q2_v2.txt"];
archivo10 = OpenWrite["Route to folder\q2_w1.txt"];
archivo11 = OpenWrite["Route to folder\q2_w2.txt"];
archivo12 = OpenWrite["Route to folder\q2_w3.txt"];
archivo13 = OpenWrite["Route to folder\q2_w4.txt"];
archivo14 = OpenWrite["Route to folder\v1_v2.txt"];
{
{archivo15 = OpenWrite["Route to folder\v1_w1.txt"]; },
{archivo16 = OpenWrite["Route to folder\v1_w2.txt"];
 archivo17 = OpenWrite["Route to folder\v1_w3.txt"];
 archivo18 = OpenWrite["Route to folder\v1_w4.txt"];
 archivo19 = OpenWrite["Route to folder\v2_w1.txt"];
 archivo20 = OpenWrite["Route to folder\v2_w2.txt"]; },
{archivo21 = OpenWrite["Route to folder\v2_w3.txt"];
 archivo22 = OpenWrite["Route to folder\v2_w4.txt"]; },
{archivo23 = OpenWrite["Route to folder\w1_w2.txt"]; },
{archivo24 = OpenWrite["Route to folder\w1_w3.txt"]; },
{archivo25 = OpenWrite["Route to folder\w1_w4.txt"];
 archivo26 = OpenWrite["Route to folder\w2_w3.txt"]; },
{archivo27 = OpenWrite["Route to folder\w2_w4.txt"];
 archivo28 = OpenWrite["Route to folder\w3_w4.txt"]; }
}
q1 = OpenRead["Route to folder\q1_alms_t1.txt"];
q2 = OpenRead["Route to folder\q2_alms_t1.txt"];
v1 = OpenRead["Route to folder\v1_alms_t1.txt"];
v2 = OpenRead["Route to folder\v2_alms_t1.txt"];
w1 = OpenRead["Route to folder\w1_alms_t1.txt"];
w2 = OpenRead["Route to folder\w2_alms_t1.txt"];
w3 = OpenRead["Route to folder\w3_alms_t1.txt"];
w4 = OpenRead["Route to folder\w4_alms_t1.txt"];
```

$$
\begin{aligned}
&\text{For}[l = 0, l<=1024, l{+}{+},\\
&\text{cl1} = 0; \text{cl2} = 0; \text{cl3} = 0; \text{cl4} = 0; \text{cl5} = 0; \text{cl6} = 0; \text{cl7} = 0;\\
&\text{cl8} = 0; \text{cl9} = 0; \text{cl10} = 0; \text{cl11} = 0; \text{cl12} = 0; \text{cl13} = 0; \text{cl14} = 0;\\
&\text{cl15} = 0; \text{cl16} = 0; \text{cl17} = 0; \text{cl18} = 0; \text{cl19} = 0; \text{cl20} = 0; \text{cl21} = 0;\\
&\text{cl22} = 0; \text{cl23} = 0; \text{cl24} = 0; \text{cl25} = 0; \text{cl26} = 0; \text{cl27} = 0;\\
&\text{cl28} = 0;\\
&\text{For}[m = 0, m<=l, m{+}{+},\\
&\text{datos1} = \text{Read}[\text{q1}, \{\text{Real}, \text{Real}, \text{Real}\}];\\
&\text{datos2} = \text{Read}[\text{q2}, \{\text{Real}, \text{Real}, \text{Real}\}];\\
&\text{datos3} = \text{Read}[\text{v1}, \{\text{Real}, \text{Real}, \text{Real}\}];\\
&\text{datos4} = \text{Read}[\text{v2}, \{\text{Real}, \text{Real}, \text{Real}\}];\\
&\text{datos5} = \text{Read}[\text{w1}, \{\text{Real}, \text{Real}, \text{Real}\}];\\
&\text{datos6} = \text{Read}[\text{w2}, \{\text{Real}, \text{Real}, \text{Real}\}];\\
&\text{datos7} = \text{Read}[\text{w3}, \{\text{Real}, \text{Real}, \text{Real}\}];\\
&\text{datos8} = \text{Read}[\text{w4}, \{\text{Real}, \text{Real}, \text{Real}\}];\\
&\text{If}\left[m{=}{=}0, \left\{\text{cl1} = \text{cl1} + \text{Abs}\left[\left(\text{datos1}_{[[2]]} + i\text{datos1}_{[[3]]}\right)\left(\text{datos2}_{[[2]]} - \text{idatos2}_{[[3]]}\right)\right]\right.\right.\\
&\text{cl2} = \text{cl2} + \text{Abs}\left[\left(\text{datos1}_{[[2]]} + \text{idatos1}_{[[3]]}\right)\left(\text{datos3}_{[[2]]} - \text{idatos3}_{[[3]]}\right)\right],\\
&\text{cl3} = \text{cl3} + \text{Abs}\left[\left(\text{datos1}_{[[2]]} + \text{idatos1}_{[[3]]}\right)\left(\text{datos4}_{[[2]]} - \text{idatos4}_{[[3]]}\right)\right],\\
&\text{cl4} = \text{cl4} + \text{Abs}\left[\left(\text{datos1}_{[[2]]} + \text{idatos1}_{[[3]]}\right)\left(\text{datos5}_{[[2]]} - \text{idatos5}_{[[3]]}\right)\right],\\
&\text{cl5} = \text{cl5} + \text{Abs}\left[\left(\text{datos1}_{[[2]]} + i\text{datos1}_{[[3]]}\right)\left(\text{datos6}_{[[2]]} - i\text{datos6}_{[[3]]}\right)\right],\\
&\text{cl6} = \text{cl6} + \text{Abs}\left[\left(\text{datos1}_{[[2]]} + i\text{datos1}_{[[3]]}\right)\left(\text{datos7}_{[[2]]} - i\text{datos7}_{[[3]]}\right)\right],\\
&\text{cl7} = \text{cl7} + \text{Abs}\left[\left(\text{datos1}_{[[2]]} + i\text{datos1}_{[[3]]}\right)\left(\text{datos8}_{[[2]]} - i\text{datos8}_{[[3]]}\right)\right],\\
&\text{cl8} = \text{cl8} + \text{Abs}\left[\left(\text{datos2}_{[[2]]} + i\text{datos2}_{[[3]]}\right)\left(\text{datos3}_{[[2]]} - i\text{datos3}_{[[3]]}\right)\right],\\
&\text{cl9} = \text{cl9} + \text{Abs}\left[\left(\text{datos2}_{[[2]]} + i\text{datos2}_{[[3]]}\right)\left(\text{datos4}_{[[2]]} - i\text{datos4}_{[[3]]}\right)\right],\\
&\text{cl10} = \text{cl10} + \text{Abs}\left[\left(\text{datos2}_{[[2]]} + i\text{datos2}_{[[3]]}\right)\left(\text{datos5}_{[[2]]} - i\text{datos5}_{[[3]]}\right)\right],\\
&\text{cl11} = \text{cl11} + \text{Abs}\left[\left(\text{datos2}_{[[2]]} + i\text{datos2}_{[[3]]}\right)\left(\text{datos6}_{[[2]]} - i\text{datos6}_{[[3]]}\right)\right],\\
&\text{cl12} = \text{cl12} + \text{Abs}\left[\left(\text{datos2}_{[[2]]} + i\text{datos2}_{[[3]]}\right)\left(\text{datos7}_{[[2]]} - i\text{datos7}_{[[3]]}\right)\right],\\
&\text{cl13} = \text{cl13} + \text{Abs}\left[\left(\text{datos2}_{[[2]]} + i\text{datos2}_{[[3]]}\right)\left(\text{datos8}_{[[2]]} - i\text{datos8}_{[[3]]}\right)\right],\\
&\text{cl14} = \text{cl14} + \text{Abs}\left[\left(\text{datos3}_{[[2]]} + i\text{datos3}_{[[3]]}\right)\left(\text{datos4}_{[[2]]} - i\text{datos4}_{[[3]]}\right)\right],\\
&\text{cl15} = \text{cl15} + \text{Abs}\left[\left(\text{datos3}_{[[2]]} + i\text{datos3}_{[[3]]}\right)\left(\text{datos5}_{[[2]]} - i\text{datos5}_{[[3]]}\right)\right],\\
&\text{cl16} = \text{cl16} + \text{Abs}\left[\left(\text{datos3}_{[[2]]} + i\text{datos3}_{[[3]]}\right)\left(\text{datos6}_{[[2]]} - i\text{datos6}_{[[3]]}\right)\right],\\
&\text{cl17} = \text{cl17} + \text{Abs}\left[\left(\text{datos3}_{[[2]]} + i\text{datos3}_{[[3]]}\right)\left(\text{datos7}_{[[2]]} - i\text{datos7}_{[[3]]}\right)\right],\\
&\text{cl18} = \text{cl18} + \text{Abs}\left[\left(\text{datos3}_{[[2]]} + i\text{datos3}_{[[3]]}\right)\left(\text{datos8}_{[[2]]} - i\text{datos8}_{[[3]]}\right)\right],\\
&\text{cl19} = \text{cl19} + \text{Abs}\left[\left(\text{datos4}_{[[2]]} + i\text{datos4}_{[[3]]}\right)\left(\text{datos5}_{[[2]]} - i\text{datos5}_{[[3]]}\right)\right],\\
&\text{cl20} = \text{cl20} + \text{Abs}\left[\left(\text{datos4}_{[[2]]} + i\text{datos4}_{[[3]]}\right)\left(\text{datos6}_{[[2]]} - i\text{datos6}_{[[3]]}\right)\right],\\
&\text{cl21} = \text{cl21} + \text{Abs}\left[\left(\text{datos4}_{[[2]]} + i\text{datos4}_{[[3]]}\right)\left(\text{datos7}_{[[2]]} - i\text{datos7}_{[[3]]}\right)\right],
\end{aligned}
$$

$$
\begin{aligned}
&\mathrm{cl22} = \mathrm{cl22} + \mathrm{Abs}\left[\left(\mathrm{datos4}_{[[2]]} + i\,\mathrm{datos4}_{[[3]]}\right)\left(\mathrm{datos8}_{[[2]]} - i\,\mathrm{datos8}_{[[3]]}\right)\right],\\
&\mathrm{cl23} = \mathrm{cl23} + \mathrm{Abs}\left[\left(\mathrm{datos5}_{[[2]]} + i\,\mathrm{datos5}_{[[3]]}\right)\left(\mathrm{datos6}_{[[2]]} - i\,\mathrm{datos6}_{[[3]]}\right)\right],\\
&\mathrm{cl24} = \mathrm{cl24} + \mathrm{Abs}\left[\left(\mathrm{datos5}_{[[2]]} + i\,\mathrm{datos5}_{[[3]]}\right)\left(\mathrm{datos7}_{[[2]]} - i\,\mathrm{datos7}_{[[3]]}\right)\right],\\
&\mathrm{cl25} = \mathrm{cl25} + \mathrm{Abs}\left[\left(\mathrm{datos5}_{[[2]]} + i\,\mathrm{datos5}_{[[3]]}\right)\left(\mathrm{datos8}_{[[2]]} - i\,\mathrm{datos8}_{[[3]]}\right)\right],\\
&\mathrm{cl26} = \mathrm{cl26} + \mathrm{Abs}\left[\left(\mathrm{datos6}_{[[2]]} + i\,\mathrm{datos6}_{[[3]]}\right)\left(\mathrm{datos7}_{[[2]]} - i\,\mathrm{datos7}_{[[3]]}\right)\right],\\
&\mathrm{cl27} = \mathrm{cl27} + \mathrm{Abs}\left[\left(\mathrm{datos6}_{[[2]]} + i\,\mathrm{datos6}_{[[3]]}\right)\left(\mathrm{datos8}_{[[2]]} - i\,\mathrm{datos8}_{[[3]]}\right)\right],\\
&\mathrm{cl28} = \mathrm{cl28} + \mathrm{Abs}\left[\left(\mathrm{datos7}_{[[2]]} + i\,\mathrm{datos7}_{[[3]]}\right)\left(\mathrm{datos8}_{[[2]]} - i\,\mathrm{datos8}_{[[3]]}\right)\right]\Big\},\\
&\Big\{\mathrm{cl1} = \mathrm{cl1} + 2\mathrm{Abs}\left[\left(\mathrm{datos1}_{[[2]]} + i\,\mathrm{datos1}_{[[3]]}\right)\left(\mathrm{datos2}_{[[2]]} - i\,\mathrm{datos2}_{[[3]]}\right)\right],\\
&\mathrm{cl2} = \mathrm{cl2} + 2\mathrm{Abs}\left[\left(\mathrm{datos1}_{[[2]]} + i\,\mathrm{datos1}_{[[3]]}\right)\left(\mathrm{datos3}_{[[2]]} - i\,\mathrm{datos3}_{[[3]]}\right)\right],\\
&\mathrm{cl3} = \mathrm{cl3} + 2\mathrm{Abs}\left[\left(\mathrm{datos1}_{[[2]]} + i\,\mathrm{datos1}_{[[3]]}\right)\left(\mathrm{datos4}_{[[2]]} - i\,\mathrm{datos4}_{[[3]]}\right)\right],\\
&\mathrm{cl4} = \mathrm{cl4} + 2\mathrm{Abs}\left[\left(\mathrm{datos1}_{[[2]]} + i\,\mathrm{datos1}_{[[3]]}\right)\left(\mathrm{datos5}_{[[2]]} - i\,\mathrm{datos5}_{[[3]]}\right)\right],\\
&\mathrm{cl5} = \mathrm{cl5} + 2\mathrm{Abs}\left[\left(\mathrm{datos1}_{[[2]]} + i\,\mathrm{datos1}_{[[3]]}\right)\left(\mathrm{datos6}_{[[2]]} - i\,\mathrm{datos6}_{[[3]]}\right)\right],\\
&\mathrm{cl6} = \mathrm{cl6} + 2\mathrm{Abs}\left[\left(\mathrm{datos1}_{[[2]]} + i\,\mathrm{datos1}_{[[3]]}\right)\left(\mathrm{datos7}_{[[2]]} - i\,\mathrm{datos7}_{[[3]]}\right)\right],\\
&\mathrm{cl7} = \mathrm{cl7} + 2\mathrm{Abs}\left[\left(\mathrm{datos1}_{[[2]]} + i\,\mathrm{datos1}_{[[3]]}\right)\left(\mathrm{datos8}_{[[2]]} - i\,\mathrm{datos8}_{[[3]]}\right)\right],\\
&\mathrm{cl8} = \mathrm{cl8} + 2\mathrm{Abs}\left[\left(\mathrm{datos2}_{[[2]]} + i\,\mathrm{datos2}_{[[3]]}\right)\left(\mathrm{datos3}_{[[2]]} - i\,\mathrm{datos3}_{[[3]]}\right)\right],\\
&\mathrm{cl9} = \mathrm{cl9} + 2\mathrm{Abs}\left[\left(\mathrm{datos2}_{[[2]]} + i\,\mathrm{datos2}_{[[3]]}\right)\left(\mathrm{datos4}_{[[2]]} - i\,\mathrm{datos4}_{[[3]]}\right)\right],\\
&\mathrm{cl10} = \mathrm{cl10} + 2\mathrm{Abs}\left[\left(\mathrm{datos2}_{[[2]]} + i\,\mathrm{datos2}_{[[3]]}\right)\left(\mathrm{datos5}_{[[2]]} - i\,\mathrm{datos5}_{[[3]]}\right)\right],\\
&\mathrm{cl11} = \mathrm{cl11} + 2\mathrm{Abs}\left[\left(\mathrm{datos2}_{[[2]]} + i\,\mathrm{datos2}_{[[3]]}\right)\left(\mathrm{datos6}_{[[2]]} - i\,\mathrm{datos6}_{[[3]]}\right)\right],\\
&\mathrm{cl12} = \mathrm{cl12} + 2\mathrm{Abs}\left[\left(\mathrm{datos2}_{[[2]]} + i\,\mathrm{datos2}_{[[3]]}\right)\left(\mathrm{datos7}_{[[2]]} - i\,\mathrm{datos7}_{[[3]]}\right)\right],\\
&\mathrm{cl13} = \mathrm{cl13} + 2\mathrm{Abs}\left[\left(\mathrm{datos2}_{[[2]]} + i\,\mathrm{datos2}_{[[3]]}\right)\left(\mathrm{datos8}_{[[2]]} - i\,\mathrm{datos8}_{[[3]]}\right)\right],\\
&\mathrm{cl14} = \mathrm{cl14} + 2\mathrm{Abs}\left[\left(\mathrm{datos3}_{[[2]]} + i\,\mathrm{datos3}_{[[3]]}\right)\left(\mathrm{datos4}_{[[2]]} - i\,\mathrm{datos4}_{[[3]]}\right)\right],\\
&\mathrm{cl15} = \mathrm{cl15} + 2\mathrm{Abs}\left[\left(\mathrm{datos3}_{[[2]]} + i\,\mathrm{datos3}_{[[3]]}\right)\left(\mathrm{datos5}_{[[2]]} - i\,\mathrm{datos5}_{[[3]]}\right)\right],\\
&\mathrm{cl16} = \mathrm{cl16} + 2\mathrm{Abs}\left[\left(\mathrm{datos3}_{[[2]]} + i\,\mathrm{datos3}_{[[3]]}\right)\left(\mathrm{datos6}_{[[2]]} - i\,\mathrm{datos6}_{[[3]]}\right)\right],\\
&\mathrm{cl17} = \mathrm{cl17} + 2\mathrm{Abs}\left[\left(\mathrm{datos3}_{[[2]]} + i\,\mathrm{datos3}_{[[3]]}\right)\left(\mathrm{datos7}_{[[2]]} - i\,\mathrm{datos7}_{[[3]]}\right)\right],\\
&\mathrm{cl18} = \mathrm{cl18} + 2\mathrm{Abs}\left[\left(\mathrm{datos3}_{[[2]]} + i\,\mathrm{datos3}_{[[3]]}\right)\left(\mathrm{datos8}_{[[2]]} - i\,\mathrm{datos8}_{[[3]]}\right)\right],\\
&\mathrm{cl19} = \mathrm{cl19} + 2\mathrm{Abs}\left[\left(\mathrm{datos4}_{[[2]]} + i\,\mathrm{datos4}_{[[3]]}\right)\left(\mathrm{datos5}_{[[2]]} - i\,\mathrm{datos5}_{[[3]]}\right)\right],\\
&\mathrm{cl20} = \mathrm{cl20} + 2\mathrm{Abs}\left[\left(\mathrm{datos4}_{[[2]]} + i\,\mathrm{datos4}_{[[3]]}\right)\left(\mathrm{datos6}_{[[2]]} - i\,\mathrm{datos6}_{[[3]]}\right)\right],\\
&\mathrm{cl21} = \mathrm{cl21} + 2\mathrm{Abs}\left[\left(\mathrm{datos4}_{[[2]]} + i\,\mathrm{datos4}_{[[3]]}\right)\left(\mathrm{datos7}_{[[2]]} - i\,\mathrm{datos7}_{[[3]]}\right)\right],\\
&\mathrm{cl22} = \mathrm{cl22} + 2\mathrm{Abs}\left[\left(\mathrm{datos4}_{[[2]]} + i\,\mathrm{datos4}_{[[3]]}\right)\left(\mathrm{datos8}_{[[2]]} - i\,\mathrm{datos8}_{[[3]]}\right)\right],\\
&\mathrm{cl23} = \mathrm{cl23} + 2\mathrm{Abs}\left[\left(\mathrm{datos5}_{[[2]]} + i\,\mathrm{datos5}_{[[3]]}\right)\left(\mathrm{datos6}_{[[2]]} - i\,\mathrm{datos6}_{[[3]]}\right)\right],\\
&\mathrm{cl24} = \mathrm{cl24} + 2\mathrm{Abs}\left[\left(\mathrm{datos5}_{[[2]]} + i\,\mathrm{datos5}_{[[3]]}\right)\left(\mathrm{datos7}_{[[2]]} - i\,\mathrm{datos7}_{[[3]]}\right)\right],\\
&\mathrm{cl25} = \mathrm{cl25} + 2\mathrm{Abs}\left[\left(\mathrm{datos5}_{[[2]]} + i\,\mathrm{datos5}_{[[3]]}\right)\left(\mathrm{datos8}_{[[2]]} - i\,\mathrm{datos8}_{[[3]]}\right)\right],\\
&\mathrm{cl26} = \mathrm{cl26} + 2\mathrm{Abs}\left[\left(\mathrm{datos6}_{[[2]]} + i\,\mathrm{datos6}_{[[3]]}\right)\left(\mathrm{datos7}_{[[2]]} - i\,\mathrm{datos7}_{[[3]]}\right)\right],\\
&\mathrm{cl27} = \mathrm{cl27} + 2\mathrm{Abs}\left[\left(\mathrm{datos6}_{[[2]]} + i\,\mathrm{datos6}_{[[3]]}\right)\left(\mathrm{datos8}_{[[2]]} - i\,\mathrm{datos8}_{[[3]]}\right)\right],\\
&\mathrm{cl28} = \mathrm{cl28} + 2\mathrm{Abs}\left[\left(\mathrm{datos7}_{[[2]]} + i\,\mathrm{datos7}_{[[3]]}\right)\left(\mathrm{datos8}_{[[2]]} - i\,\mathrm{datos8}_{[[3]]}\right)\right]\Big\}\Big]
\end{aligned}
$$

```
 ];
Write[archivo1, {l, 1/(2l + 1)cl1}];
Write[archivo2, {l, 1/(2l + 1)cl2}];
Write[archivo3, {l, 1/(2l + 1)cl3}];
Write[archivo4, {l, 1/(2l + 1)cl4}];
Write[archivo5, {l, 1/(2l + 1)cl5}];
Write[archivo6, {l, 1/(2l + 1)cl6}];
Write[archivo7, {l, 1/(2l + 1)cl7}];
Write[archivo8, {l, 1/(2l + 1)cl8}];
Write[archivo9, {l, 1/(2l + 1)cl9}];
Write[archivo10, {l, 1/(2l + 1)cl10}];
Write[archivo11, {l, 1/(2l + 1)cl11}];
Write[archivo12, {l, 1/(2l + 1)cl12}];
Write[archivo13, {l, 1/(2l + 1)cl13}];
Write[archivo14, {l, 1/(2l + 1)cl14}];
Write[archivo15, {l, 1/(2l + 1)cl15}];
Write[archivo16, {l, 1/(2l + 1)cl16}];
Write[archivo17, {l, 1/(2l + 1)cl17}];
Write[archivo18, {l, 1/(2l + 1)cl18}];
Write[archivo19, {l, 1/(2l + 1)cl19}];
Write[archivo20, {l, 1/(2l + 1)cl20}];
Write[archivo21, {l, 1/(2l + 1)cl21}];
Write[archivo22, {l, 1/(2l + 1)cl22}];
Write[archivo23, {l, 1/(2l + 1)cl23}];
Write[archivo24, {l, 1/(2l + 1)cl24}];
Write[archivo25, {l, 1/(2l + 1)cl25}];
Write[archivo26, {l, 1/(2l + 1)cl26}];
Write[archivo27, {l, 1/(2l + 1)cl27}];
Write[archivo28, {l, 1/(2l + 1)cl28}];

]
```

Bibliography

[1] Carroll, B.W. and Ostlie D.A. An Introduction to Modern Astrophysics. Addison-Wesley Publishing, c1996.

[2] C.L. Bennett, et al. First Year Wilkinson microwave Anisotropy Probe (WMAP) Observations: Foreground Emission. 2003,ApJS.

[3] Dept. Physics & Astronomy University of Tennessee. Astronomy 161 *The Solar System*. Consulted on September 2007. http://csep10.phys.utk.edu/astr161/lect/time/coordinates.html

[4] Górski, K.M., E. Hivon, A.J. Banday, B.D. Wandelt, F.K. Hansen, M. Reinecke, and M. Bartelmann, HEALPix: A Framework for High-resolution Discretization and Fast Analysis of Data Distributed on the Sphere, Ap.J., 622, 759-771, 2005.

[5] Górski, K.M., E. Hivon, A.J. Banday, B.D. Wandelt, F.K. Hansen, The HEALPix Primer, Version 2.00, August 31,2005.

[6] Gurzadyan V. G., Kocharyan A. A. Paradigms of the Large-Scale Universe, CRC Press, 1994. Available in electronic form at http://books.google.com/books?id=4cIcmQfeSYEC&printsec=frontcover&dq=Paradigms+of+the+Large-Scale+Universe&hl=es&sig=6LtNine1hryPCY4Z5hnliiLwQFg#PPP1,M1

[7] Hinshaw G., et al. First Year Wilkinson Microwave Anisotropy Probe (WMAP) Observations: The Angular Power Spectrum. 2003, ApJS.

[8] Hivon Eric, Hansen Frode K., Wandelt Benjamin D., G´orski Krzysztof M., Banday Anthony J., Reinecke Martin. HEALPix Fortran Facility User Guidelines. Version 2.00; August 31, 2005.

[9] Lachièze Marc and Gunzig Edgard, The Cosmological Background Radiation, Cambrige University Press, 1999.

[10] Liddle Andrew, An Introduction to Modern Cosmology, Wiley, Second Edition, 2003.

[11] Liddle Andrew, Lyth David. Cosmological Inflation and Large-Scale Structure. Cambridge University Press. 2000.

[12] NASA. Goddard Space Flight Center, Smithsonian Astrophysical Observatory. Consulted on August of 2007. http://fits.gsfc.nasa.gov/

[13] NASA. Goddard Space Flight Center, Smithsonian Astrophysical Observatory. Consulted on August of 2007. http://heasarc.gsfc.nasa.gov/docs/heasarc/fits.html

[14] NASA. Jet Propulsion Laboratory, California Insitute of Technology. Consulted on August of 2007. http://healpix.jpl.nasa.gov/

[15] NASA. Legacy Archive for Microwave Background Data Analysis. Consulted on April 2007. http://lambda.gsfc.nasa.gov/product/map/current/m_products.cfm

[16] NASA. Legacy Archive for Microwave Background Data Analysis. Consulted on October 2007. http://lambda.gsfc.nasa.gov/product/map/current/map_images/f02_int_mask_b.png

[17] NASA. Wilkinson Microwave Anisotropy Probe. Consulted on October 10 of 2007. http://map.gsfc.nasa.gov/m_ig.html

[18] NASA. Wilkinson Microwave Anisotropy Probe. Consulted on October 10 of 2007. http://map.gsfc.nasa.gov/m_mm.html

[19] NASA. Wilkinson Microwave Anisotropy Probe. Consulted on October 10 of 2007. http://map.gsfc.nasa.gov/m__mm/ob_tech1.html

[20] NASA. Wilkinson Microwave Anisotropy Probe. Consulted on October 10 of 2007. http://map.gsfc.nasa.gov/m_mm/ob_techfreq.html

[21] NASA. Wilkinson Microwave Anisotropy Probe. Consulted on October 10 of 2007. http://map.gsfc.nasa.gov/m_mm/ob_techoptics.html

[22] NASA. Wilkinson Microwave Anisotropy Probe. Consulted on October 10 of 2007. http://map.gsfc.nasa.gov/m_mm/ob_techorbit1.html

[23] NASA. Wilkinson Microwave Anisotropy Probe. Consulted on October 10 of 2007. http://map.gsfc.nasa.gov/m_mm/ob_techradiometers.html

[24] NASA. Wilkinson Microwave Anisotropy Probe. Consulted on October 10 of 2007. http://map.gsfc.nasa.gov/m_mm/ob_techscan.html

[25] Public Broadcasting Service. NOVA Online. Consulted on August 2007. http://www.pbs.org/wgbh/nova/universe/historysans.html

[26] Ryden Barabara,Introduction to Cosmology. Addison Wesley, 2003.

[27] Silk, Joseph. The Big Bang, 3rd edition. Henry Holt and Company, LLC, 2002.

[28] Vista Collaborative Arts. Consulted on August 2007. http://www.vista-arts.com/media/images/immersive_images/vista_web_big_bang_1.jpg

[29] Wikipedia, The Free Encyclopedia. Consulted on October of 2007. http://upload.wikimedia.org/wikipedia/commons/9/98/End_of_universe.jpg

[30] Wikipedia, The Free Encyclopedia. Consulted on October of 2007. http://upload.wikimedia.org/wikipedia/en/8/8a/Electromagnetic-Spectrum.png

[31] Wilkinson Microwave Anisotropy Probe (WMAP): Explanatory Supplement, editor M. Limon, et al (Greenbelt, MD: NASA/GSFC) Available in electronic form at http://lambda.gsfc.nasa.gov